

The P2 and MOLLER Experiments: Setup and Measurement Techniques for High Precision Tests of the Running of the Weak Mixing Angle.

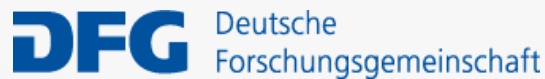
Mainz, MESA facility CRC Kickoff meeting.
Johannes Gutenberg Universität

Michael Gericke



For the P2 and MOLLER Collaborations

With grateful acknowledgement of the support provided by these funding agencies:



Office of Science

Personal Introduction:

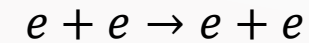
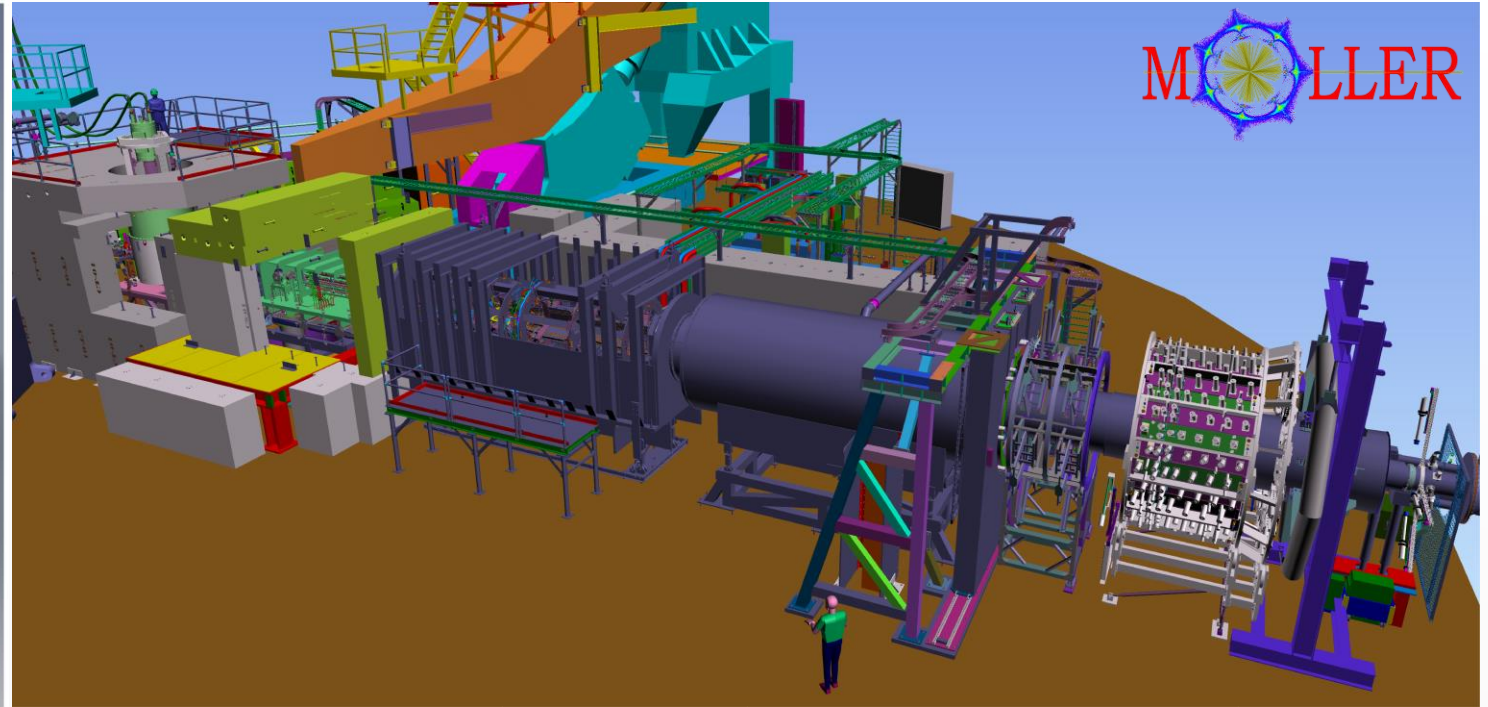
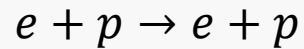
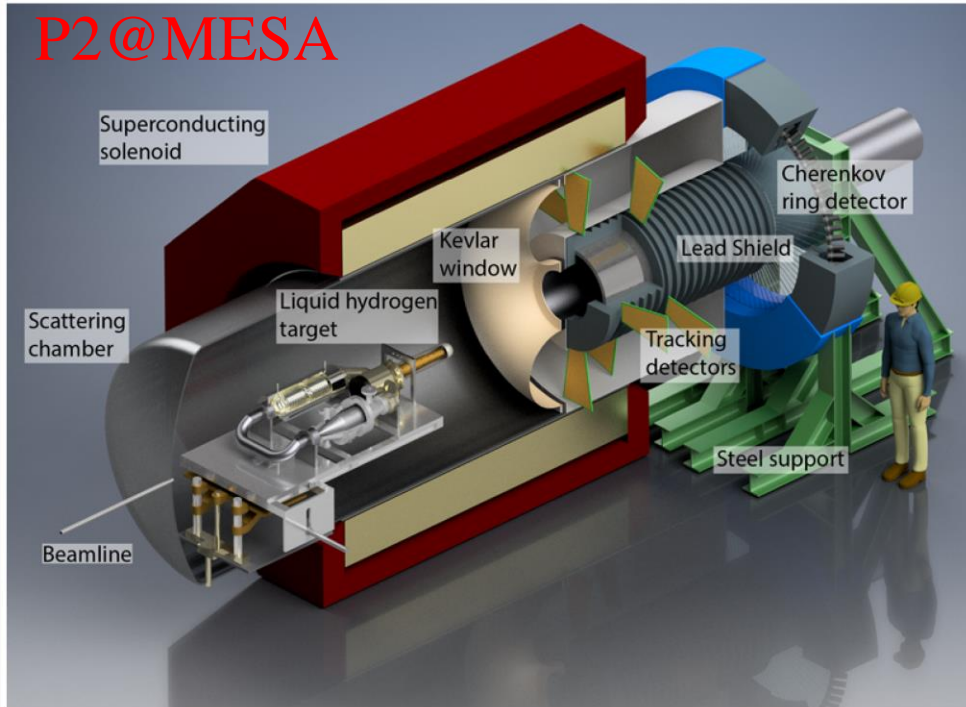
- Graduate education (M.Sc. , Ph.D.): Indiana University – Graduate research assistant at LANL 2001-2004
 - Cold neutron physics (In Memoriam: John David Bowman (LANL and ORNL) † 07.11.2024)
 - NPDGamma experiment: Parity violation in neutron-proton capture - construction of CsI(Tl) detector array and integration mode readout electronics
- Postdoctoral research: TRIUMF (BC, Canada) and Jefferson Lab (USA) 2004-2007
 - Parity violating electron scattering
 - GZero experiment: Strange quark contribution to nucleon form factors - construction of the back-angle pion veto aerogel Cherenkov detectors
 - QWeak experiment: P2 predecessor - detector development, simulations and first prototypes
 - MOLLER experiment: First detector simulations and conceptual design
 - Cold neutron physics
 - parity violation in neutron-proton capture ($n^3\text{He}$ experiment proposal development)
 - parity violation in neutron-proton capture (NPDGamma move to ORNL)
 - neutron beta decay (Nab experiment at ORNL proposal development)

Personal Introduction:

- Assistant Professor: University of Manitoba (Canada) 2007-2012
 - GZero back-angle data production
 - QWeak construction (joint responsibility for construction of the main detectors)
 - NPDGamma data production
 - $n^3\text{He}$ development and construction (responsible for ^3He ion-chamber active target-detector)
 - Nab – beta decay silicon detector development and testing
 - MOLLER R&D and proposal development
 - Ultra-cold neutron physics (nEDM) at TRIUMF (proposal development and R&D)
- Associate Professor: University of Manitoba (Canada) 2012-2018
 - QWeak data production
 - $n^3\text{He}$ data production
 - MOLLER R&D
 - P2 development (my participation started around 2015)
 - Nab – beta decay silicon detector development and testing
 - Ultra-cold neutron physics (nEDM) at TRIUMF (detector prototyping)
- Professor: University of Manitoba (Canada) 2018 – present
 - MOLLER R&D and construction
 - P2 R&D and construction (electronics)
 - Nab construction and data production (only minor contributions now)
 - Ultra-cold neutron physics (nEDM) at TRIUMF (not currently very active)

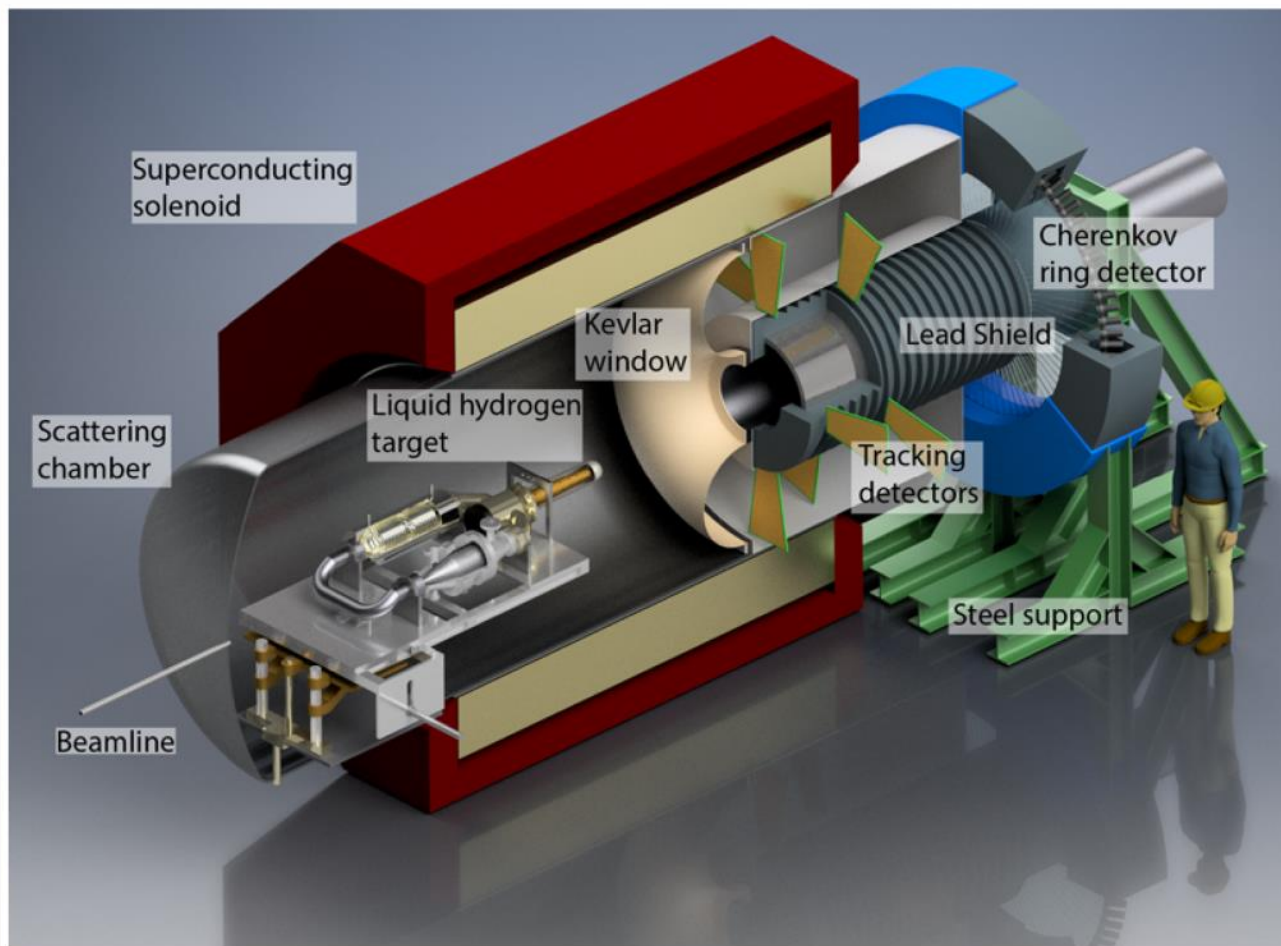
Personal Introduction:

My main efforts are now on the MOLLER and P2 experiments:



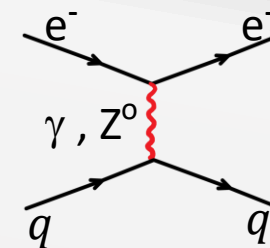
Both experiments are now in their respective construction phase and there has been a great amount of synergy and collaboration between the two efforts during the R&D stage (with hugely important contributions from the Mainz group toward MOLLER).

The P2 Experiment (Mainz MESA Facility)



Main Observable:
PV asymmetry with detectors
Weak Charge of the proton

$$A_{PV} = \frac{G_F Q^2}{4\sqrt{2} \pi\alpha} \left(Q_W^e - F(Q^2) \right)$$



$$E_{beam} = 155 \text{ MeV}$$

$$I_{beam} = 150 \mu\text{A}$$

$$\mathcal{L} = 2.4 \times 10^{39} \text{ cm}^{-2} \cdot \text{s}^{-1}$$

$$P_{beam} \geq 80 \pm 0.4 \%$$

$$A_{PV} = -40 \text{ ppb}$$

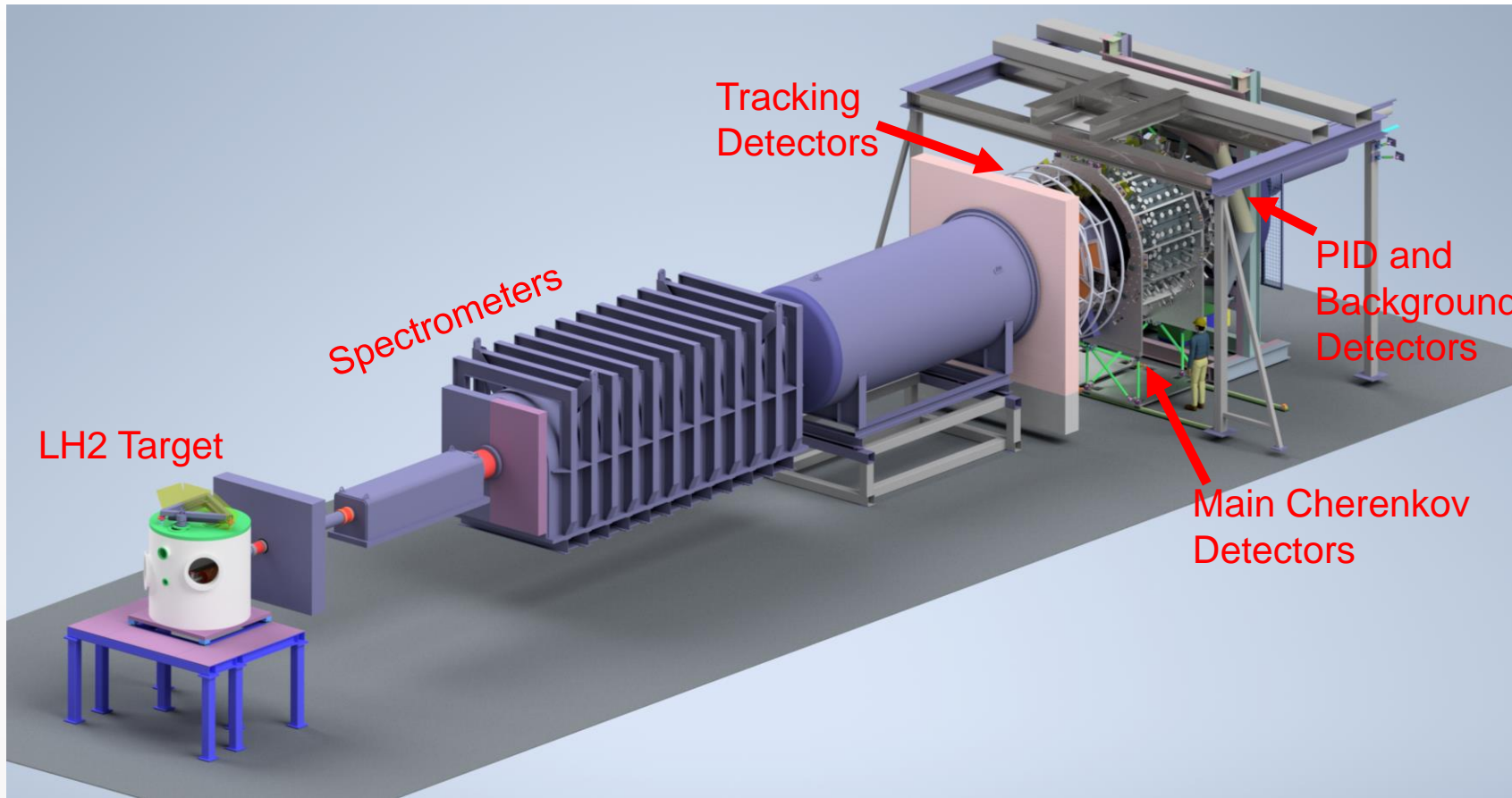
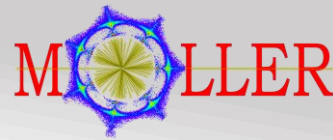
$$\delta A_{PV} = 0.6 \text{ ppb}$$

$$Q_W^p = (1 - 4\sin^2\theta_W)$$

$$\Delta Q_W^p = 1.83\%$$

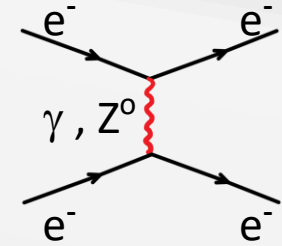
$$\Delta\sin^2\theta_W = 0.14\%$$

The MOLLER experiment (Jefferson Lab)



Main Observable:
PV asymmetry with detectors
Weak Charge of the electron

$$A_{PV} = m_e E \frac{G_F}{\pi \alpha \sqrt{2}} \frac{4 \sin^2 \theta}{(3 + \cos^2 \theta)^2} Q_W^e$$



$$E_{beam} = 11 \text{ GeV}$$

$$I_{beam} = 65 \mu\text{A}$$

$$\mathcal{L} = 3 \times 10^{39} \text{ cm}^{-2} \cdot \text{s}^{-1}$$

$$2.75 \leq E_{scat} \leq 8.25 \text{ GeV}$$

$$P_{beam} \geq 90 \pm 0.5 \%$$

$$A_{PV} = 32 \text{ ppb}$$

$$\delta A_{PV} = 0.8 \text{ ppb}$$

$$Q_W^e = -(1 - 4 \sin^2 \theta_W)$$

$$\Delta Q_W^e = 2.4\%$$

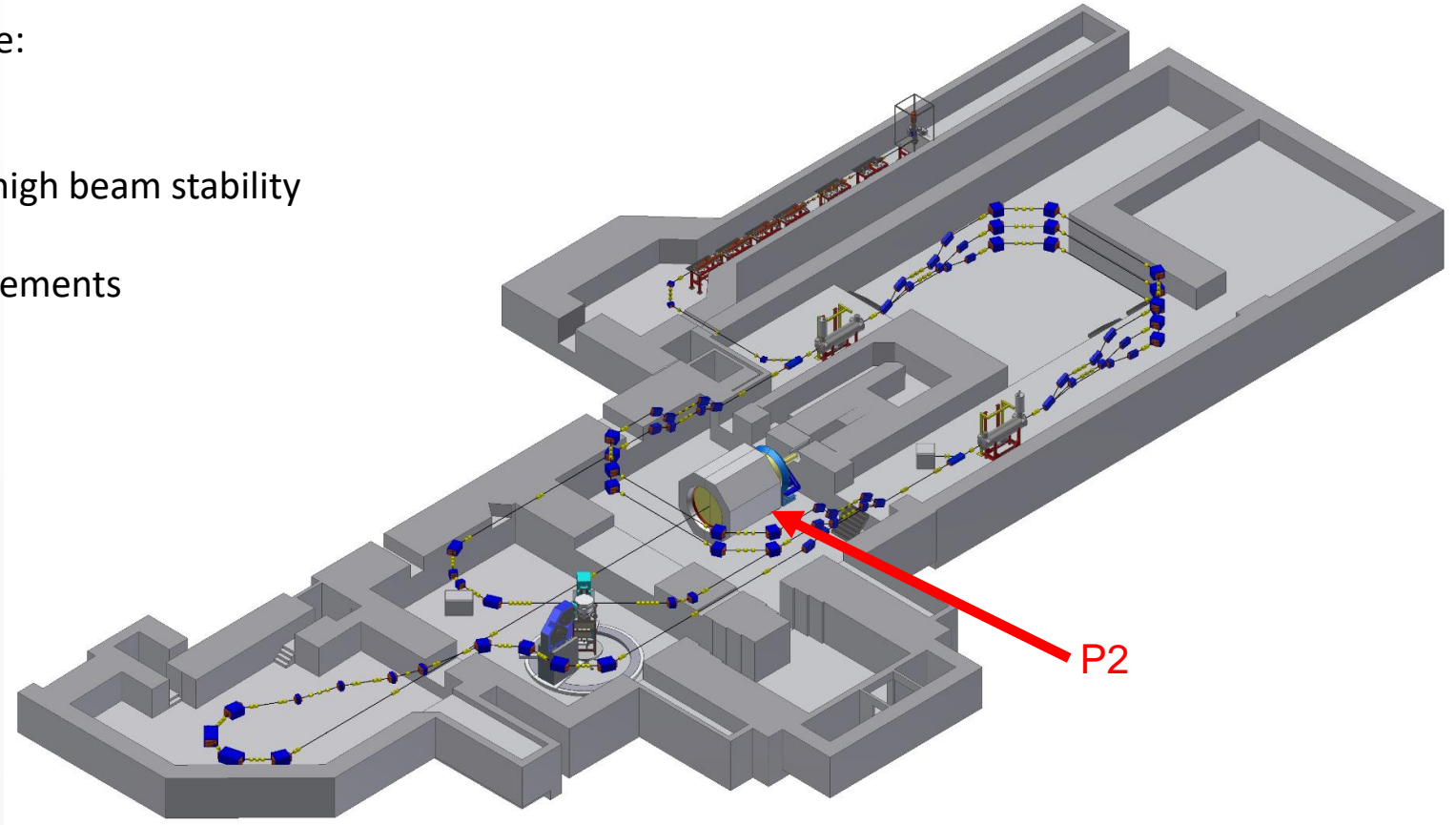
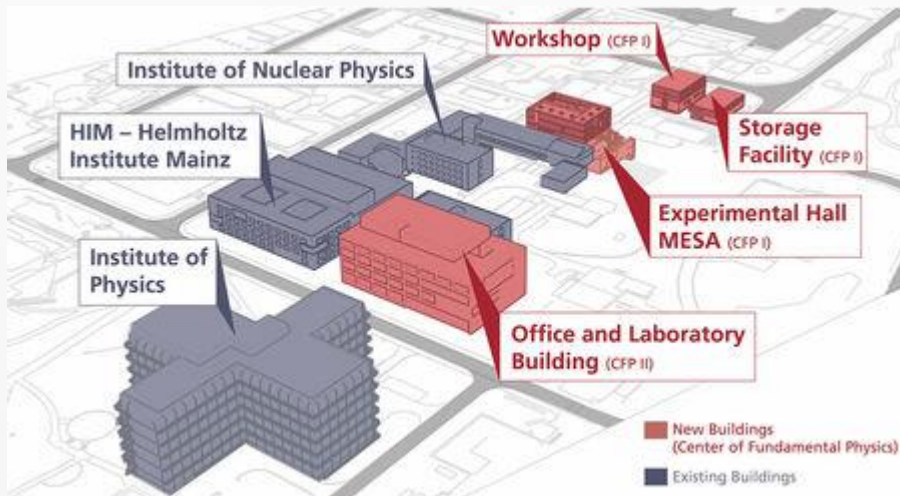
$$\Delta \sin^2 \theta_W = 0.1\%$$

The P2 Experiment (Mainz MESA Facility)

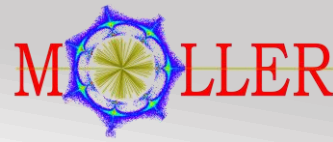
P2 will run at the New MESA Facility, Mainz, Germany making use of the high intensity electron beam with the highest possible electron beam polarization.

Particular beam properties that are important include:

- High luminosity
- Parity quality beam: High polarization with high beam stability and systematic control
- Highest precision beam polarimetry measurements
- High power LH2 target



The MOLLER experiment (Jefferson Lab)



MOLLER will run at the Thomas Jefferson National Accelerator Facility, Virginia, USA making use of the high intensity high energy electron beam with the highest possible electron beam polarization.

The experiment will be located in hall A, the largest of the 4 halls.

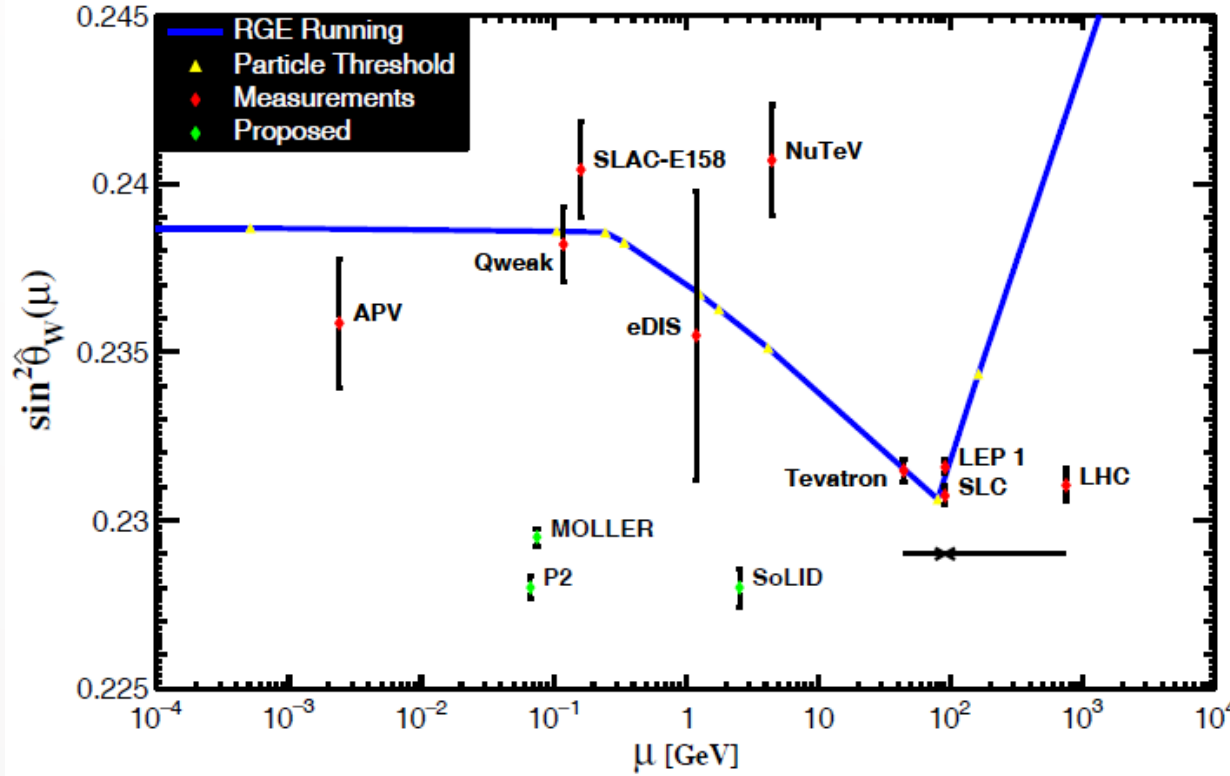
Particular beam properties that are important include:

- High luminosity
- Parity quality beam: High polarization with high beam stability and systematic control
- High precision beam polarimetry measurements
- High power LH2 target

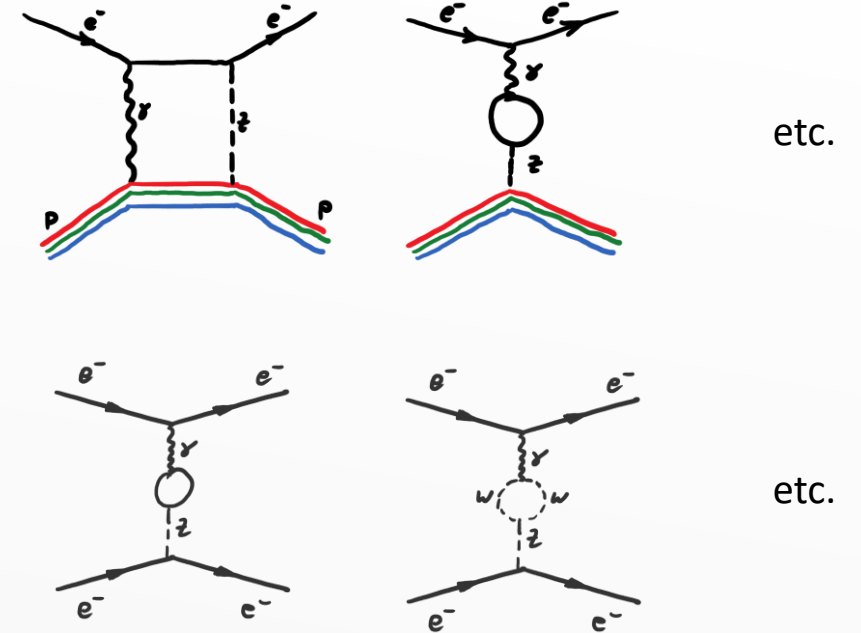


The Weak Mixing Angle

J. Erler (JGU), reproduced with permission



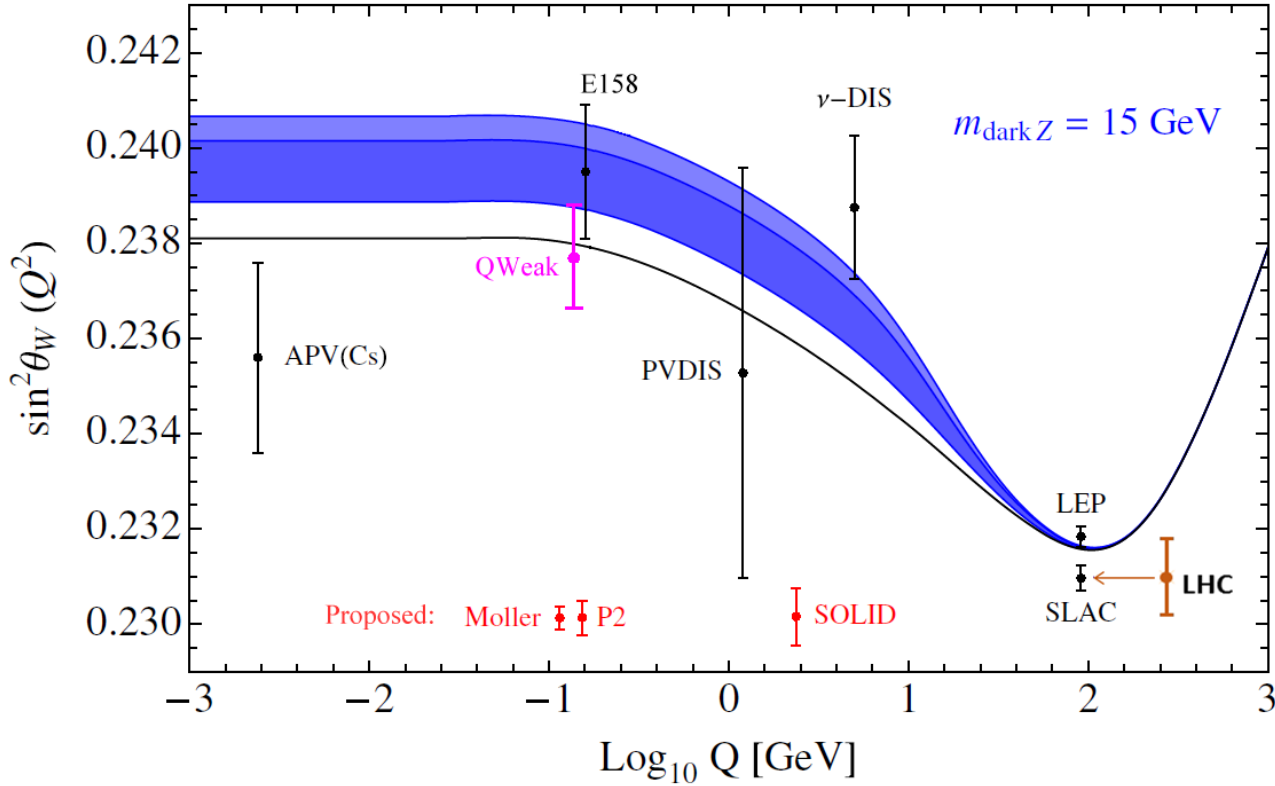
The weak mixing angle changes (“running”) with interaction energy (e.g. momentum transfer), due to:



Different radiative correction apply to different particle interactions (e.g. electron with electrons vs. electron with quarks).

The Weak Mixing Angle and New Physics

Adapted from Davoudiasl et al. PRD 92, 055005 (2015)

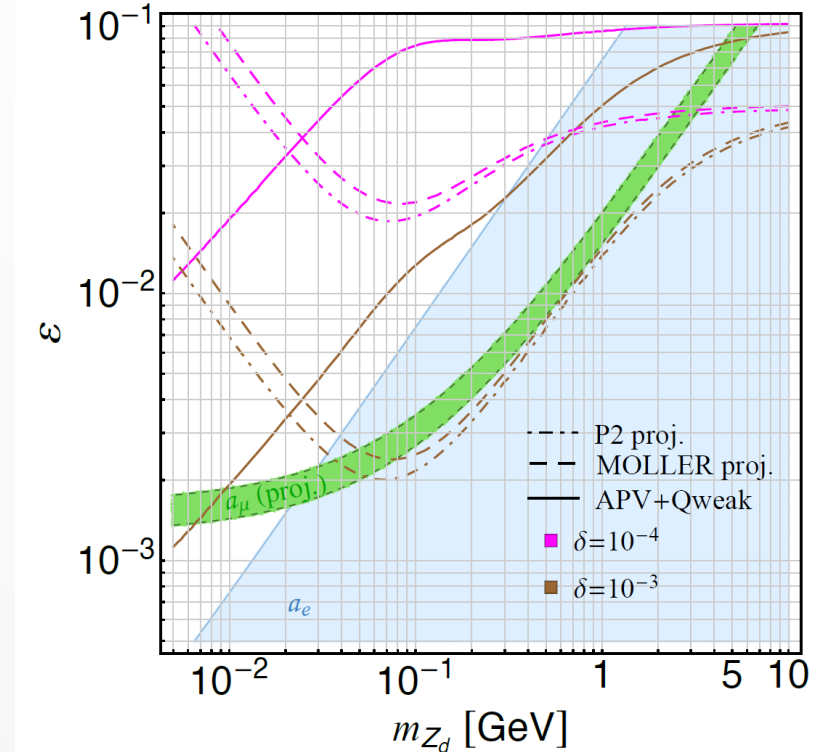


The running of the weak mixing angle away from the Z-Pole would change with the addition new physics models.

Dark matter Z bosons with different mass would produce different levels of deviation from the Standard Model prediction

$$\sin^2(\hat{\theta}_W) \rightarrow \kappa_d \sin^2(\hat{\theta}_W)$$

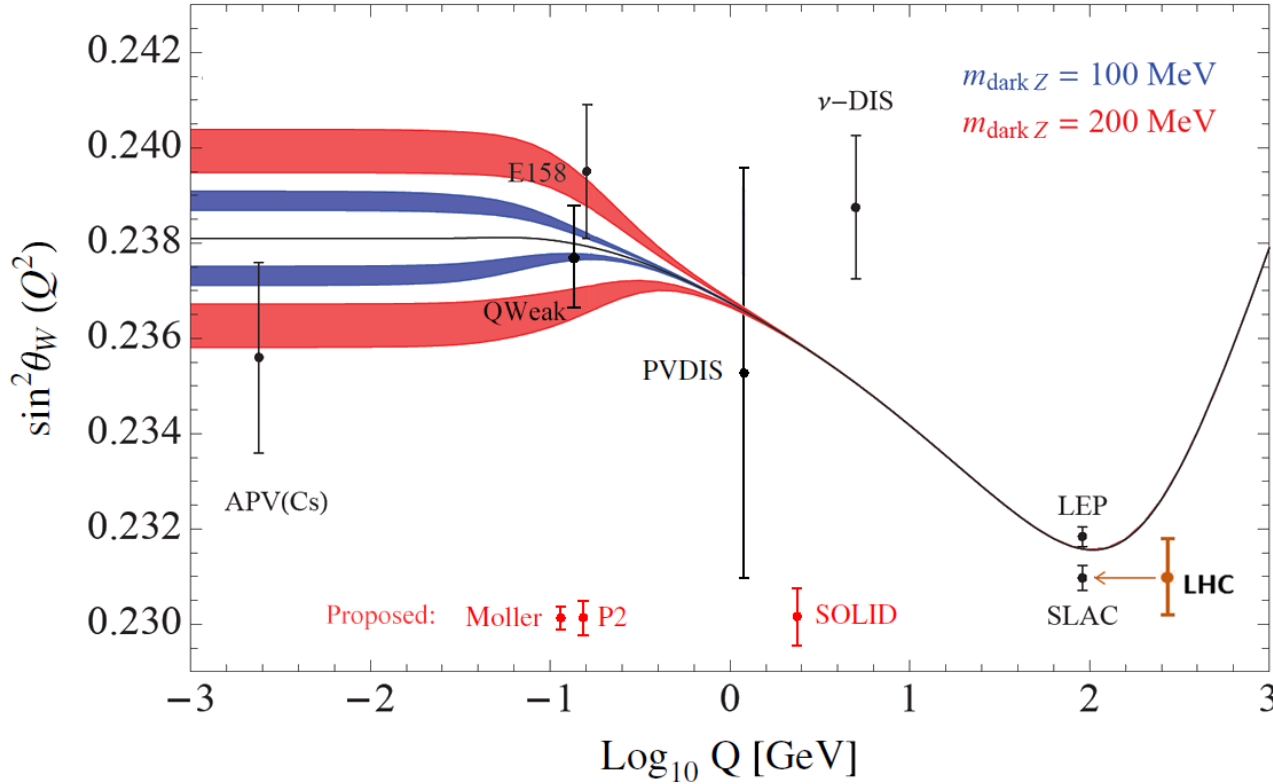
$$\kappa_d = 1 - \epsilon \left(\frac{m_Z}{m_{Z_d}} \delta + \epsilon \tan(\hat{\theta}_W) \right) \cot(\hat{\theta}_W) f \left(\frac{Q^2}{m_{Z_d}^2} \right)$$



M. Cadeddu et al. arXiv:2104.03280v3 [hep-ph]

The Weak Mixing Angle and New Physics

Adapted from Marciano, Davoudiasl, Lee (2014)

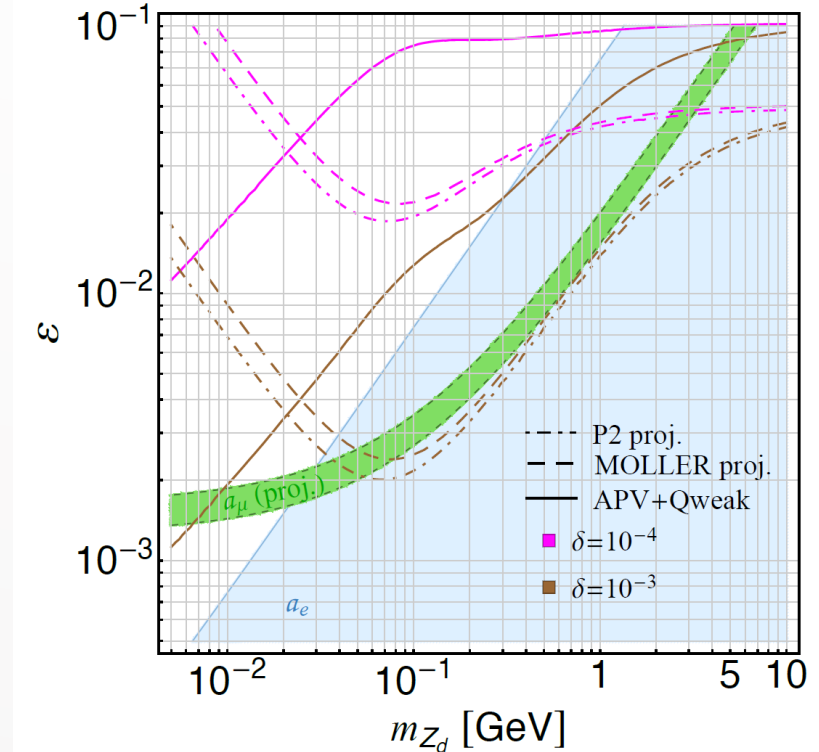


The running of the weak mixing angle away from the Z-Pole would change with the addition new physics models.

Dark matter Z bosons with different mass would produce different levels of deviation from the Standard Model prediction

$$\sin^2(\hat{\theta}_W) \rightarrow \kappa_d \sin^2(\hat{\theta}_W)$$

$$\kappa_d = 1 - \epsilon \left(\frac{m_Z}{m_{Z_d}} \delta + \epsilon \tan(\hat{\theta}_W) \right) \cot(\hat{\theta}_W) f \left(\frac{Q^2}{m_{Z_d}^2} \right)$$



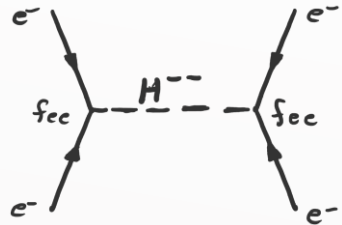
M. Cadeddu et al. arXiv:2104.03280v3 [hep-ph]

The Weak Mixing Angle and New Physics

P. S. Bhupal Dev, et al. PysRev D 98, 055013 (2018)

Additional physics sensitivities include:

- Type II seesaw neutrino mass motivated doubly charged scalars



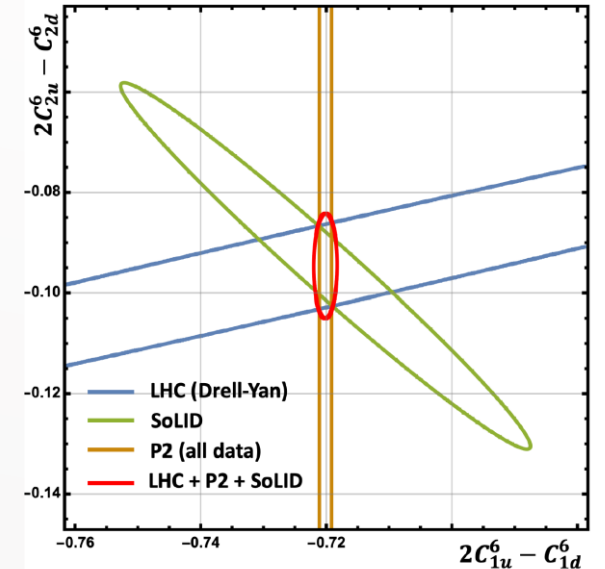
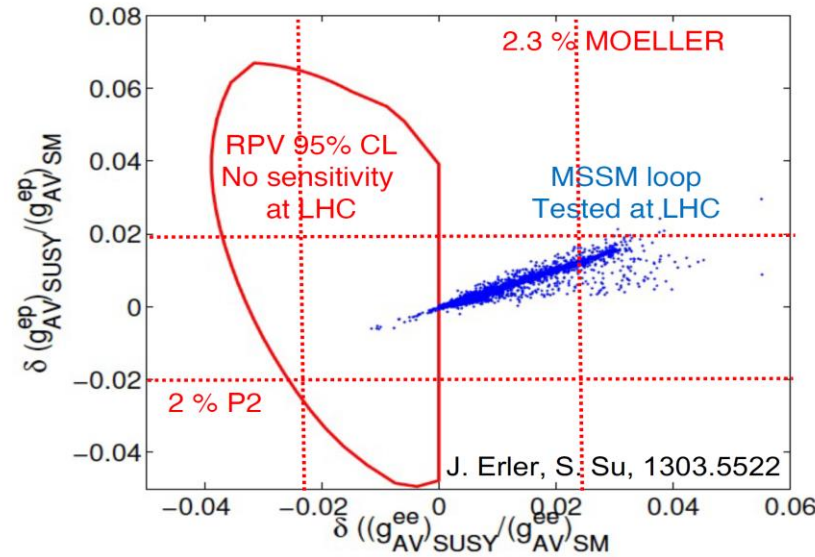
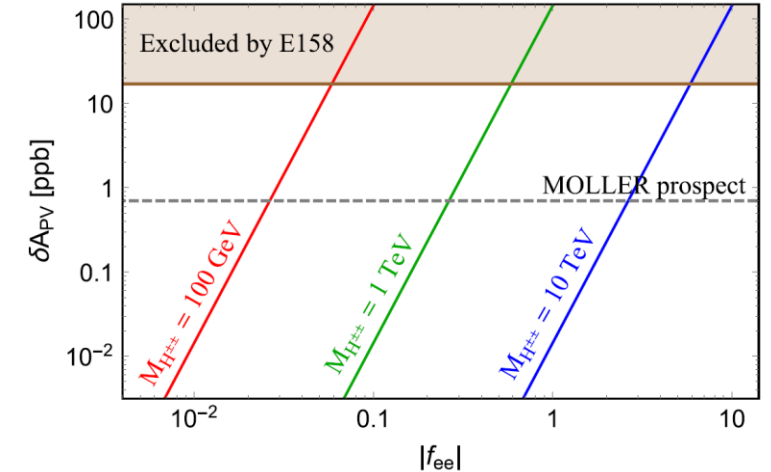
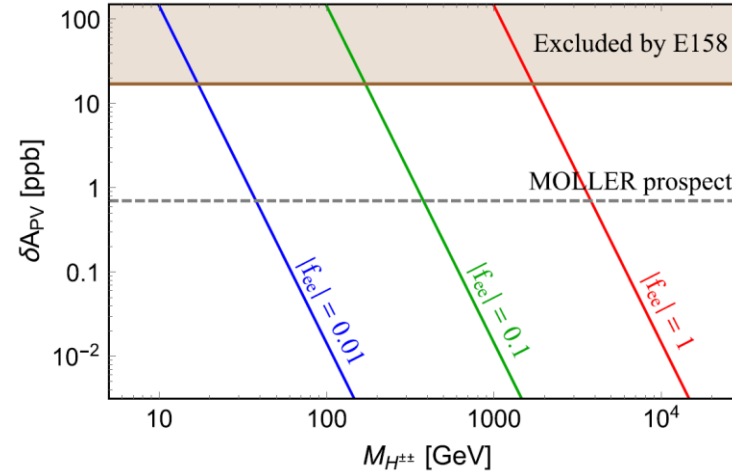
- R-Parity Violating SUSY

- New contact interactions

$$\mathcal{L}_{e_1 e_2} = \sum_{i,j=LR} \frac{g_{ij}}{2\Lambda^2} \bar{e}_i \gamma_\mu e_i \bar{e}_j \gamma^\mu e_j$$

$$\frac{\Lambda}{\sqrt{|g_{RR}^2 - g_{LL}^2|}} = 7.5 \text{ TeV}$$

- Lepton Compositeness (up to 50 TeV)
- SMEFT constraints for dim 6 operators

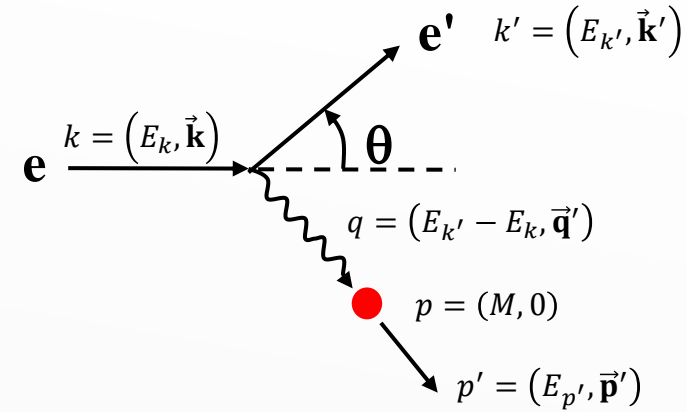


R. Boughezal et al., arXiv:2104.03979v1 [hep-ph]

Measurement Methodology

Both experiments will measure the asymmetry in the number of scattered electrons as a function of beam helicity.

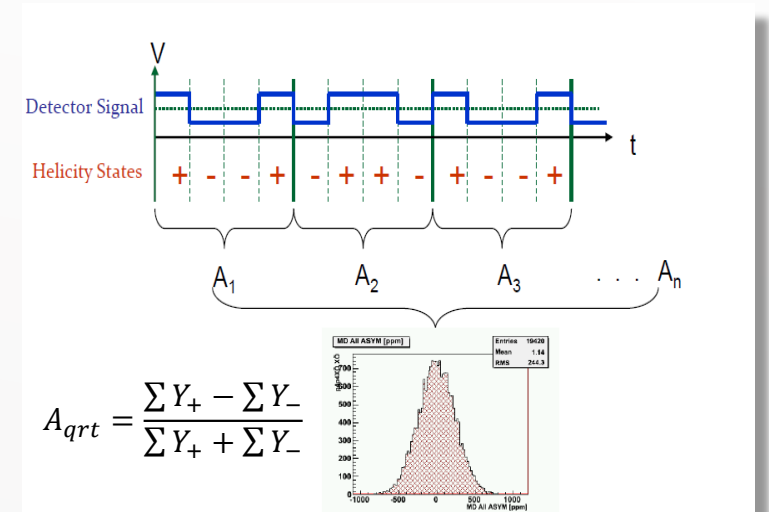
$$A = \frac{\sigma_L - \sigma_R}{\sigma_L + \sigma_R}$$



The measured flux will be integrated (both spatially and in time) over the helicity window, to form the measured asymmetry at the pair, quartet, or octet level.

All systematic effect must be taken into account:

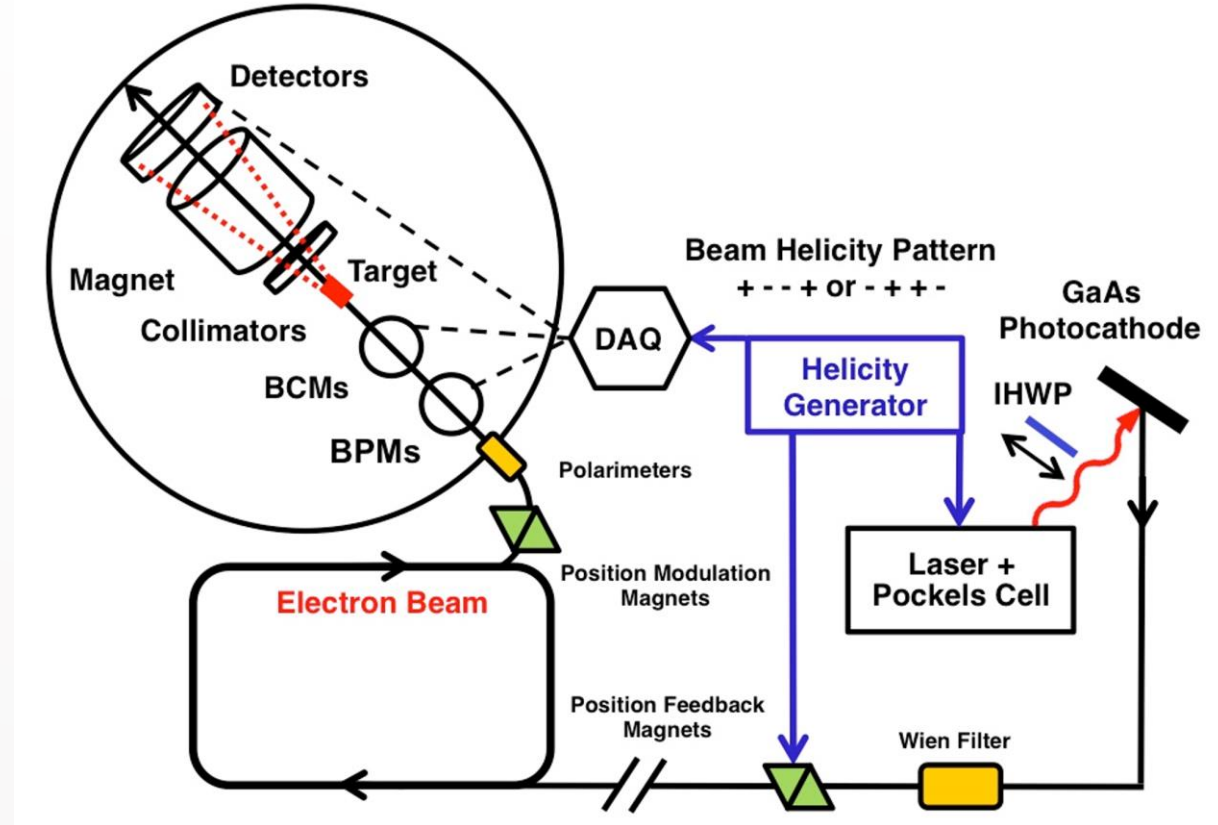
$$A_{msr} = \frac{Y^+ - Y^-}{Y^+ + Y^-} = P_e \left(f_p A_{PV} + \sum_b A_b f_b \right) + A_{beam} + A_{inst}$$



Measurement Methodology

We need multiple pieces of instrumentation, before the target.

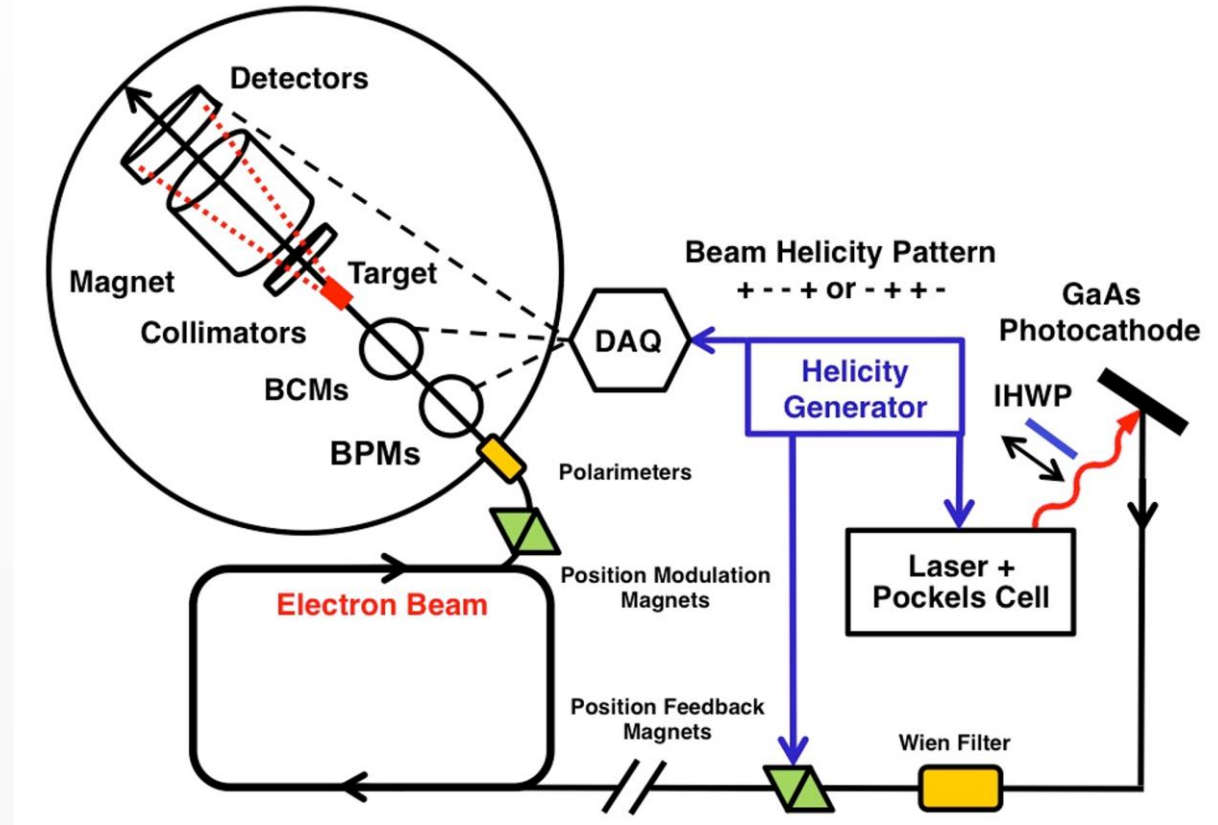
- **Helicity Generator:** Everything is synched to this frequency, defining the integration window.
- **Laser and Pockels cell:** Allowing rapid reversal of helicity, preferably with minimum deadtime (ringing) between stable helicity states.
- **Source Photocathode:** High efficiency electron source – beam spot movable.
- **Helicity Reversal:** Several ways to reverse the beam helicity (fast and slow).
- **Beam Monitoring:** Beam position (BPM) and beam current (BCM) measurements.
- **Beam Modulation and Feedback:** Move (modulate) the beam to study false asymmetries. Feedback on BM data to stabilize beam.



Measurement Methodology

We ideally have three independent techniques for helicity reversal of a longitudinally polarized beam:

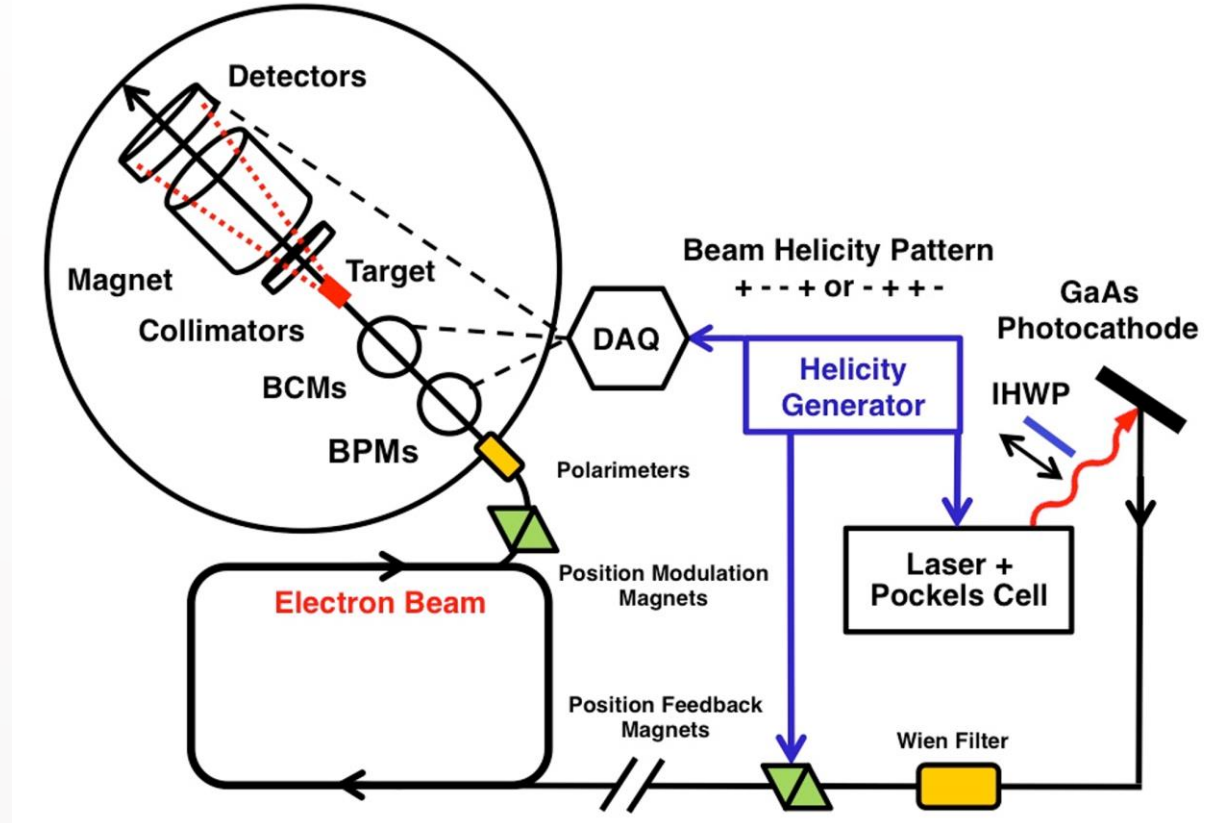
- **Rapid pseudo-random reversal:** (~ 1 kHz).
Rejects LH2 target “boiling noise”.
- **IHWP at ~ 8 -hour intervals:** Mechanical action unable to induce electrical or magnetic induced false asymmetries.
- **Wien filter at monthly intervals:** Rejection of beam size (or focus) modulation induced false asymmetry and suppression of slow drifts in apparatus linearity.
- **Also as check construct NULL:** “out-of-phase” quantity from the two slow reversal techniques to bound unaccounted for false asymmetries.



Measurement Methodology

Main experimental components:

- **Target:** High power capable (high beam currents) LH2 target with low target boiling.
- **Collimation:** Define the acceptance of the experiment.
- **Magnet:** Not really a spectrometer – used to “focus” the scattered electrons on the detectors, maximizing event rate (at the chosen kinematics). Reject background events.
- **Detectors:** Experiment needs to run in two modes: data production in integration mode and tracking for kinematics determination and background/efficiency checks. Requires two different sets of detectors (tracking and integration). Set of auxiliary detectors for systematics and monitoring.
- **Data acquisition:** High precision, low noise data acquisition integrated accurately in the helicity synchronization. Low noise amplifiers - linear electronics - fast, high-resolution ADCs.

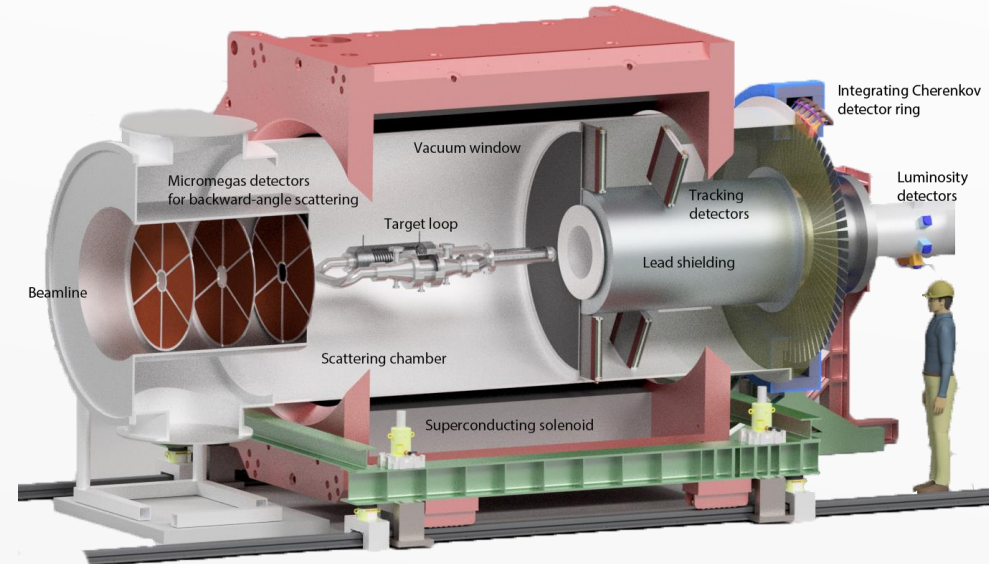
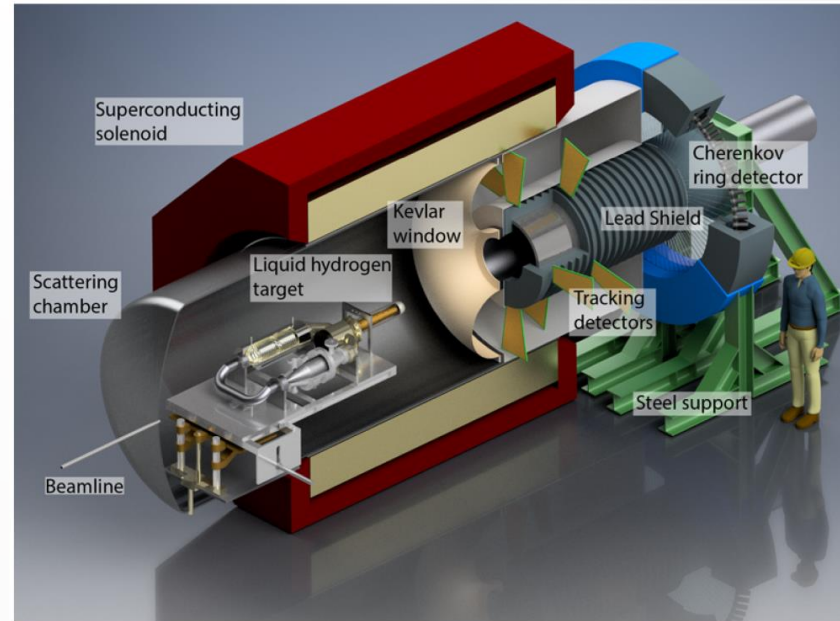


The P2 Experiment

$$A_{msr} = P_e \left(f_p A_{pV} + \sum_b A_b f_b \right) + A_{beam} + A_{inst}$$

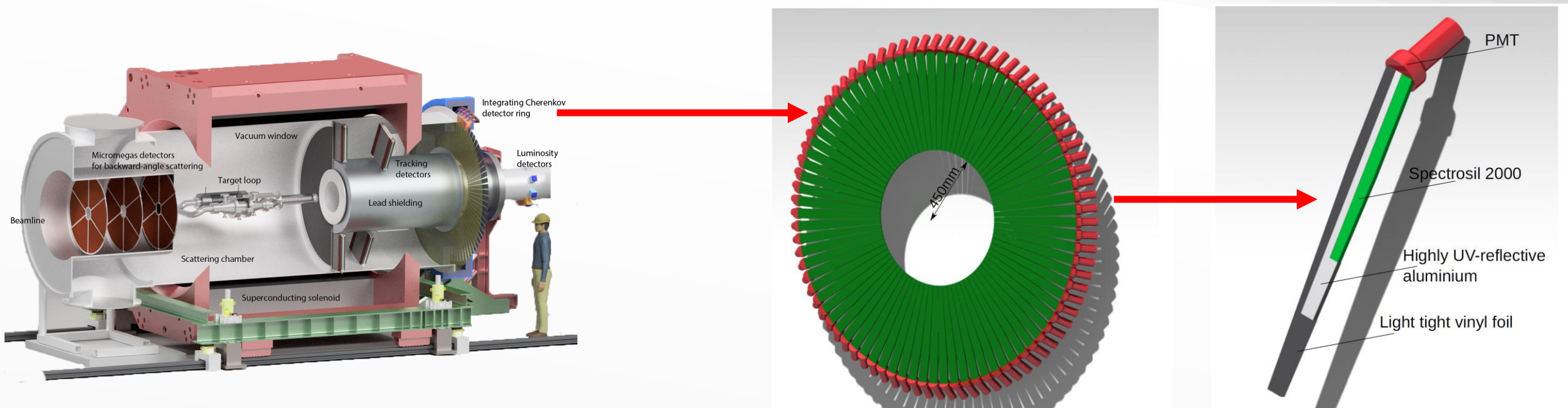
$$A_{pV} = \frac{G_F Q^2}{4\sqrt{2} \pi \alpha} (Q_W^e - F(Q^2))$$

P_e = electron polarization
 f_p = flux fraction from desired physics signal
 f_b = flux fraction from background signal
 A_{pV} = physics asymmetry
 A_b = background asymmetries
 A_{inst} = instrumental (false) asymmetries
 Q^2 = momentum transfer



The P2 Experiment

Figures and photos from the Mainz P2 group

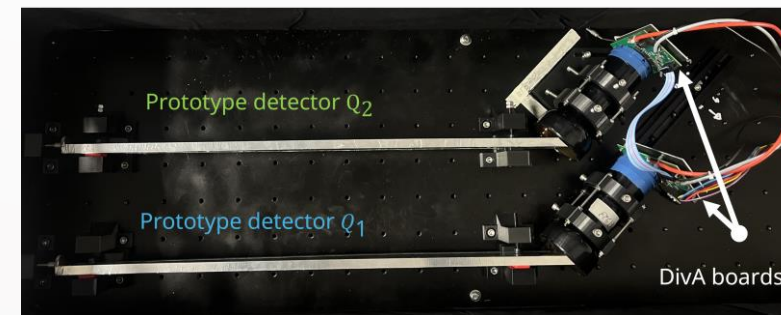
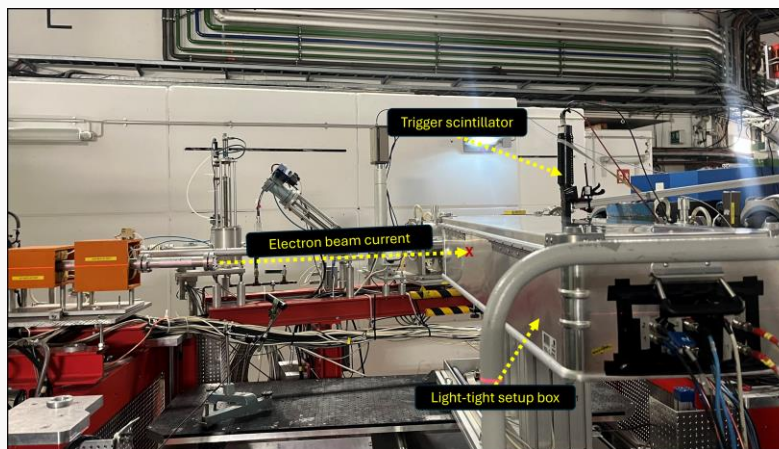


The main Cherenkov detectors measure the physics asymmetry.

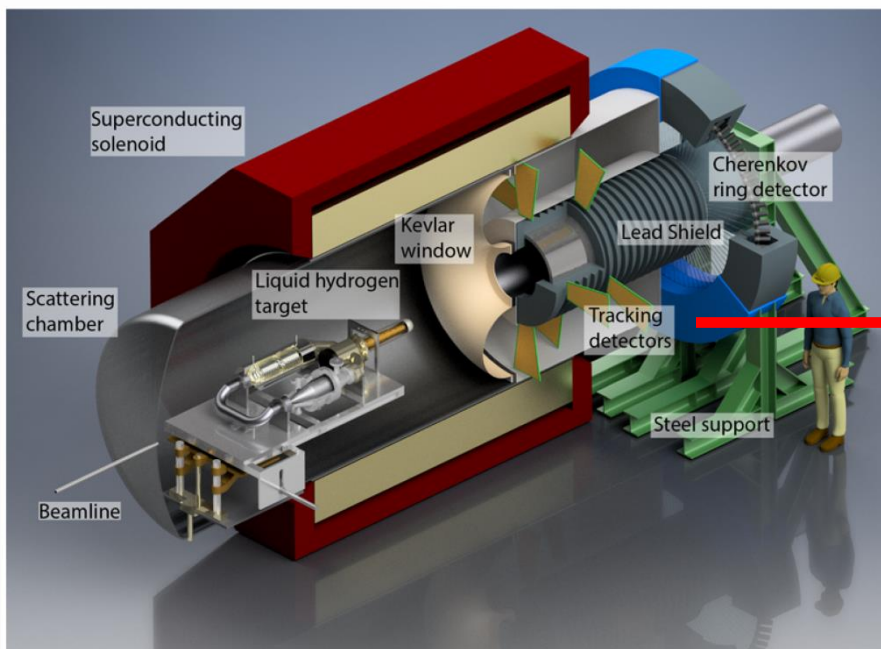
Using 72, 65 cm long, highly fused silica bars

Total internal reflection of signal light, guided to PMT

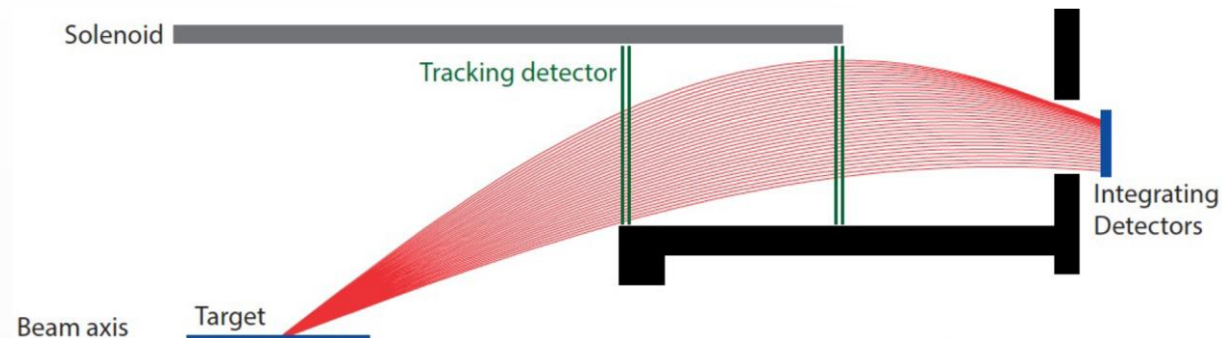
Use low noise integrating electronics (UofM contribution)



The P2 Experiment



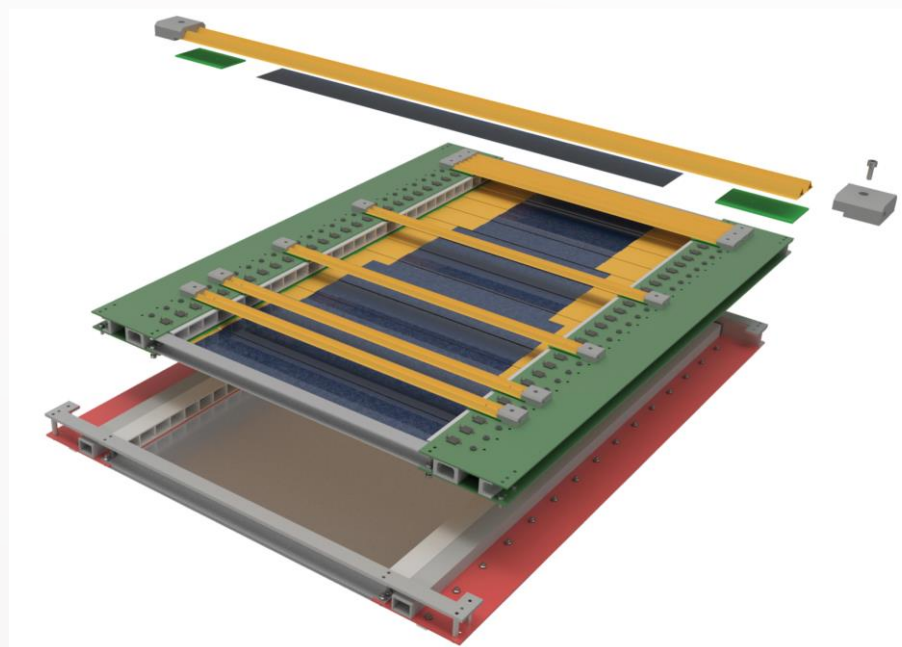
Figures and photos from the P2 CDR

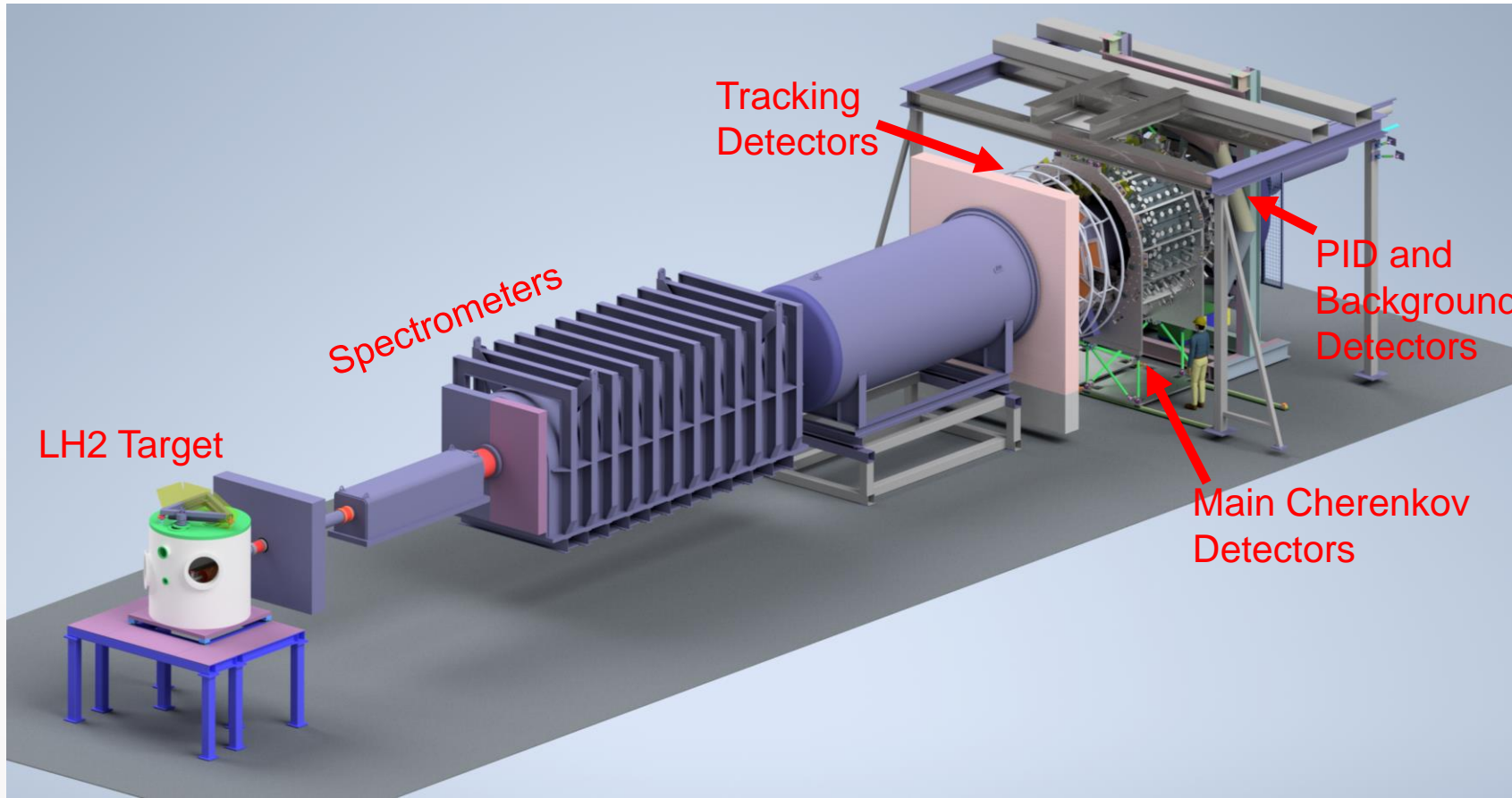


The tracking detectors measure the momentum transfer and possible backgrounds

Using two planes of multiple, large area, tiled HVMAPS (P2Pix - MuPix chip adaptation)

- Primarily Nik Berger's group
- Adaptation in MOLLER profile monitor
- Small UofM contributions to P2 sensor implementation





P_e = electron polarization
 f_p = flux fraction from desired physics signal
 f_b = flux fraction from background signal
 A_{pV} = physics asymmetry
 A_b = background asymmetries
 A_{inst} = instrumental (false) asymmetries

The event rate in the detector is Q^2 dependent, but the asymmetry is not.

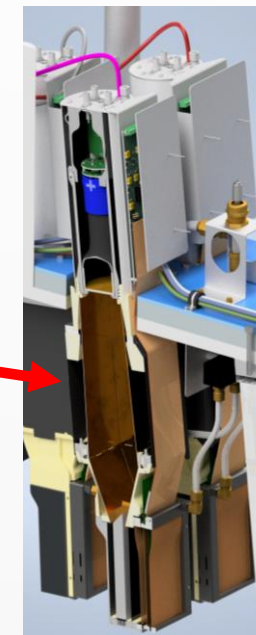
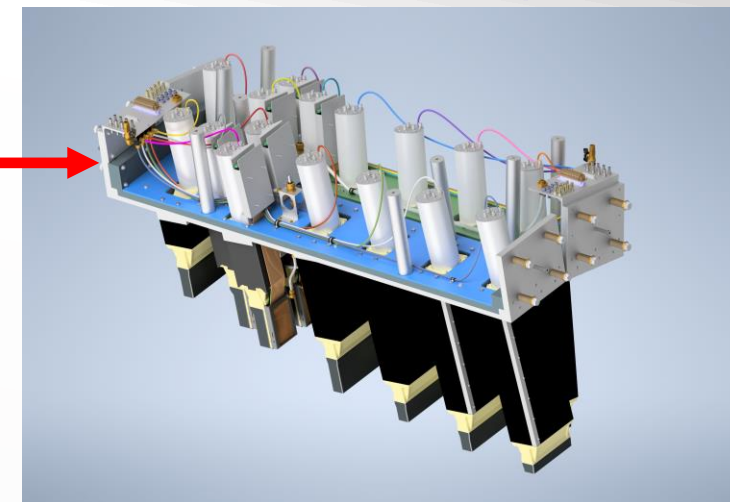
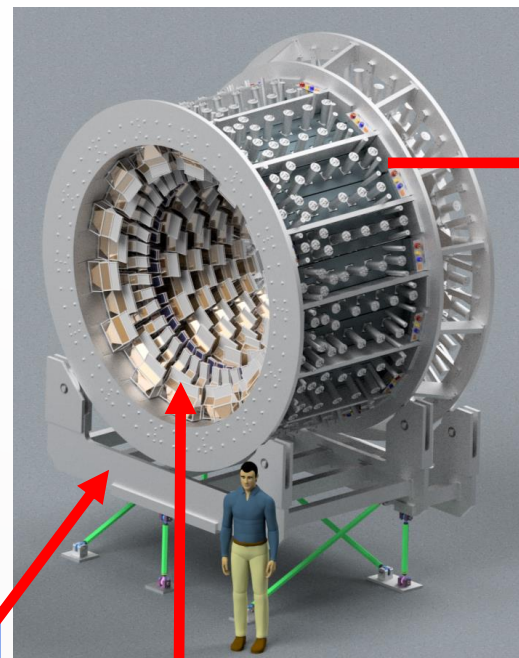
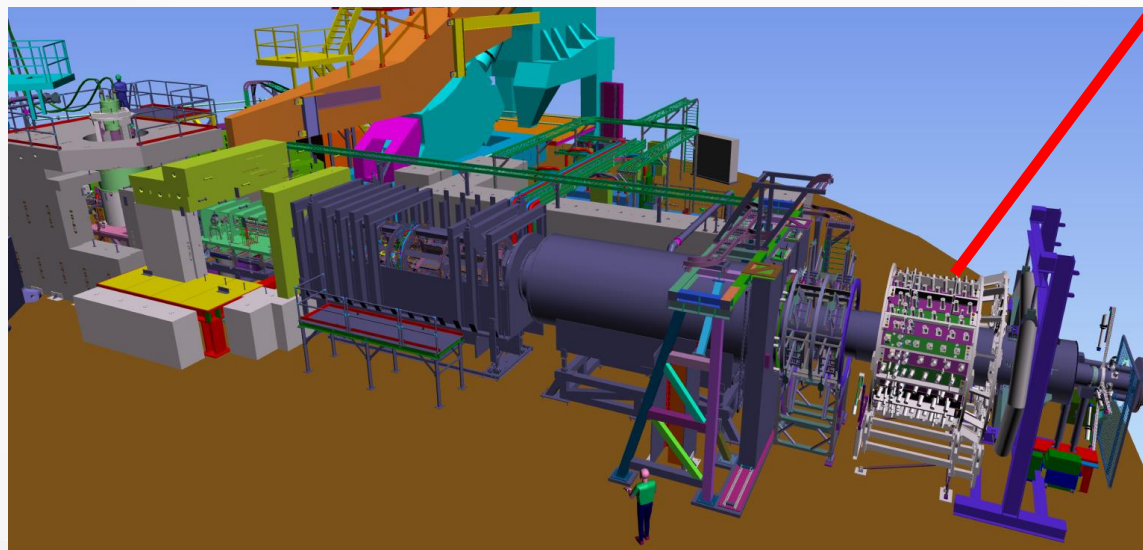
$$A_{msr} = P_e \left(f_p A_{pV} + \sum_b A_b f_b \right) + A_{beam} + A_{inst}$$

$$A_{pV} = mE \frac{G_F}{\sqrt{2}\pi\alpha} \frac{4 \sin^2 \theta}{(3 + \cos^2 \theta)^2} Q_W^e$$

MOLLER Experiment

The integrating detector package consists of 252 separate detector modules and electronics, including (\$6M funding package by the Canada Foundation for Innovation):

1. Mounting structure
2. Quartz active material
3. Light guide
4. Photo-multiplier tube and base
5. Preamplifier
6. ADC
7. Cabling, Power Supplies, etc.
8. Cooling/dry air flushing



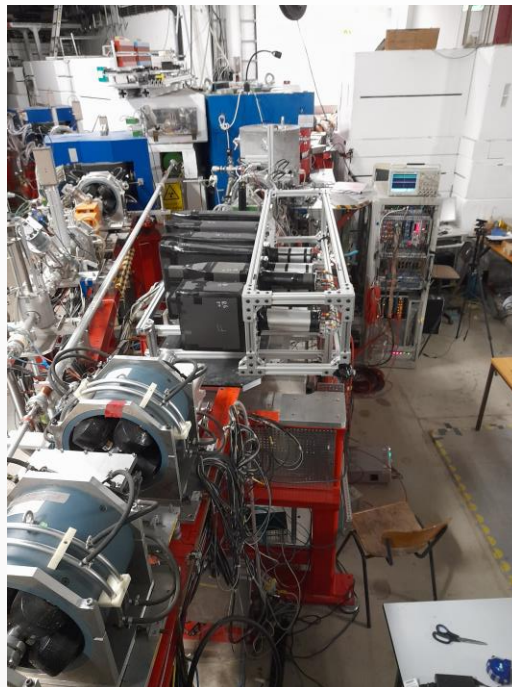
Ring 5: 84 detectors - quartz /HVMAPS combination

Other rings: 140 detectors - quartz only

MOLLER Experiment

The integrating detector package consists of 252 separate detector modules and electronics, including (\$6M funding package by the Canada Foundation for Innovation):

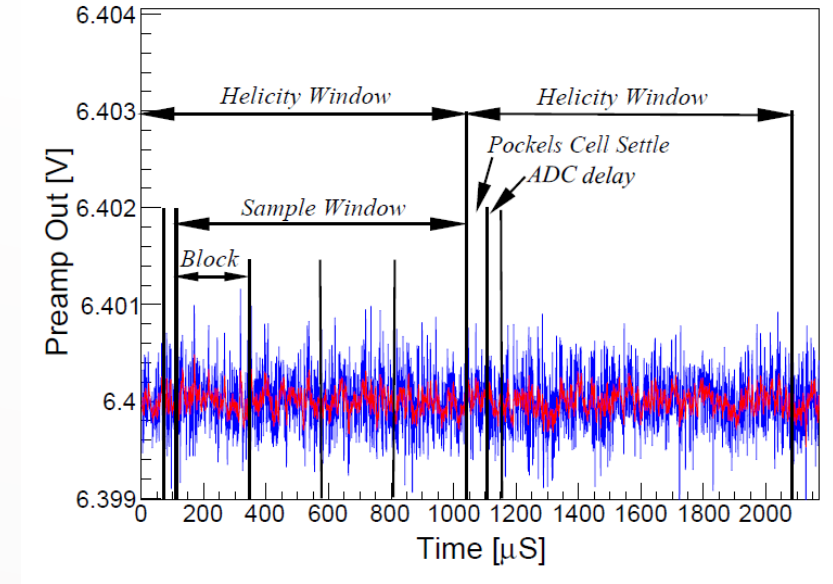
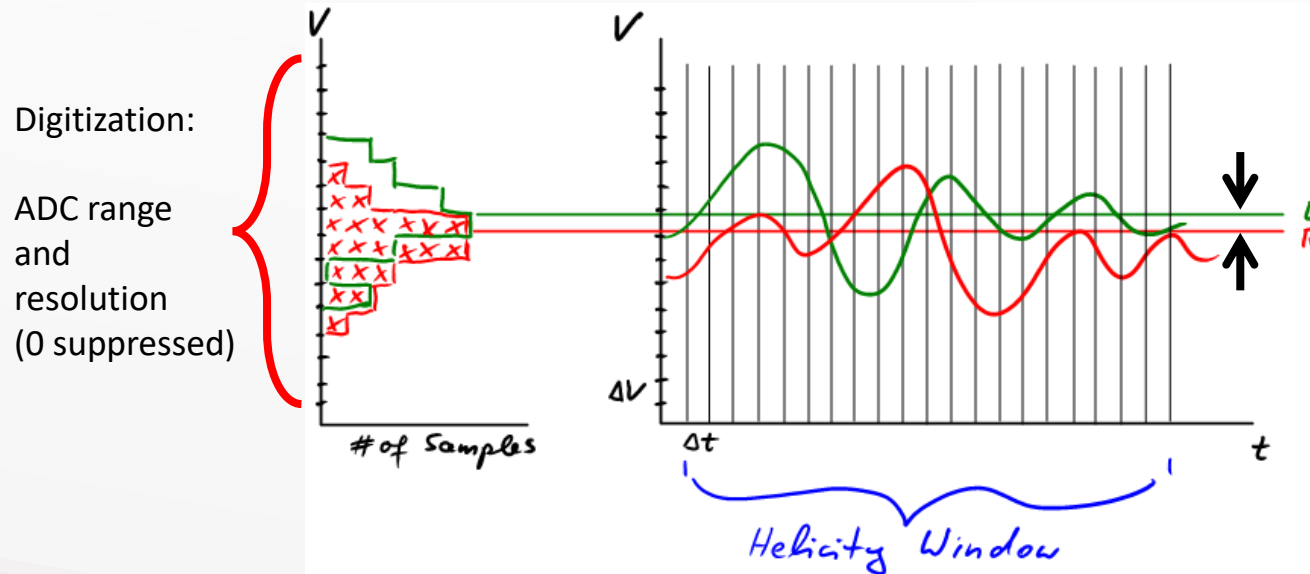
1. Mounting structure
2. Quartz active material
3. Light guide
4. Photo-multiplier tube and base
5. Preamplifier
6. ADC
7. Cabling, Power Supplies, etc.
8. Cooling/dry air flushing



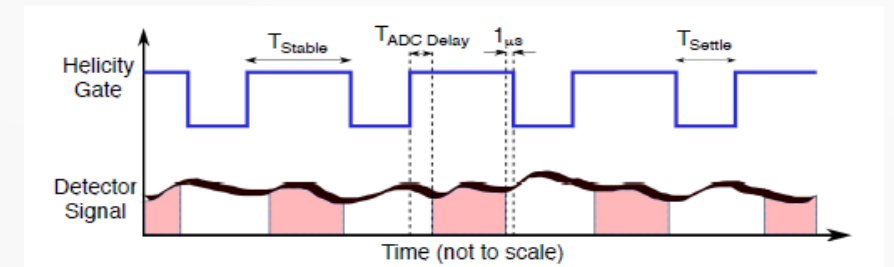
Integration Mode Front-end Electronics Design (My contribution to P2):

ADC Operating Principle:

- Trying to measure a ~ 30 ppb asymmetry $\Delta V \approx 0.12 \mu V @ 2V$
- Optimize parameters: PMT signal, ADC range, resolution (timing and amplitude)
- Selected ADC: 18 bit, 15 Msps ($\sim 14\,705\,882$ Hz actual)
- Dynamic range: ± 4.096 V
- Amplitude resolution: $\approx 4V/2^{17} \approx 32 \mu V$
- Massively over-sample within each helicity window



$\approx 0.12 \mu V @ 2V$



Integration Mode Front-end Electronics Design (My contribution to P2):

Data acquisition components for integration mode running

- Two main components:
 - ADC board
 - Trigger interface/distribution
- Each ADC board serves as a trigger slave, receiving clock synchronization, run start, and helicity flip signals
- The trigger interface card can be configured as master or slave
- The master TI receives clock sync and run start/stop (sync_res) and helicity trigger signals from the helicity generator.
- TI slaves cards receive signals from the master card and distribute further to the ADC boards.
- ADC boards sample and sum signals between helicity triggers and collect timestamp information.

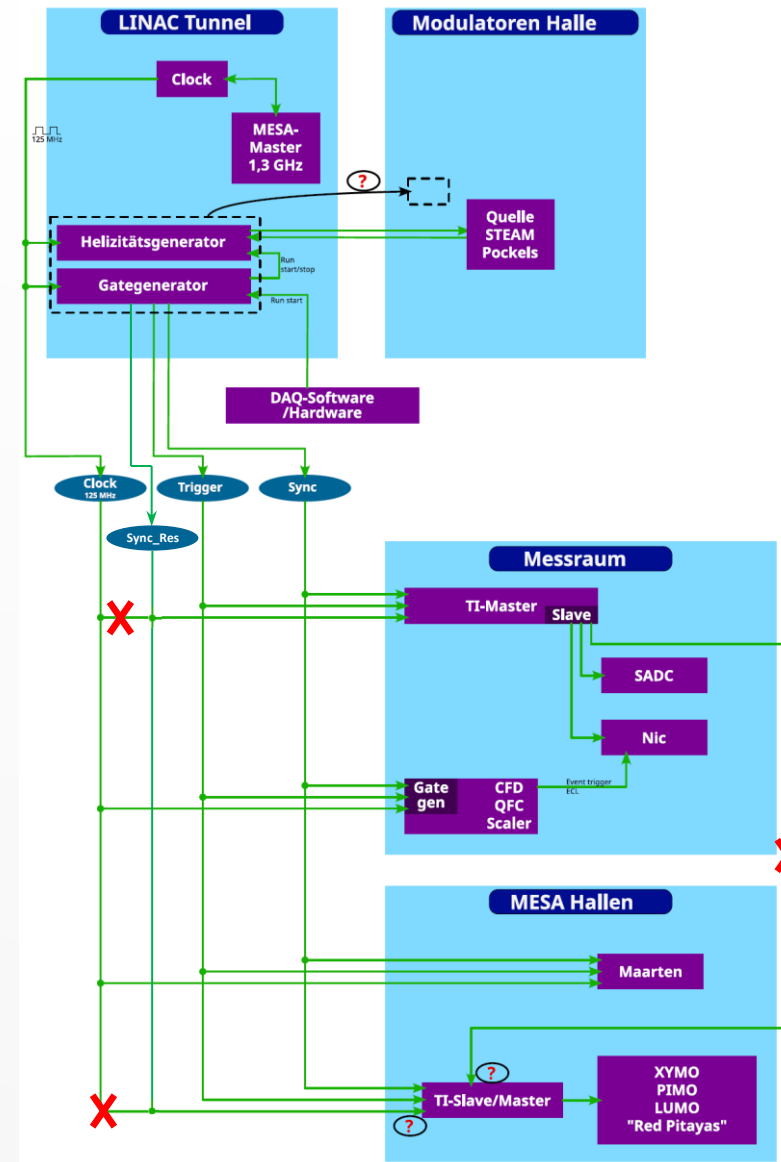
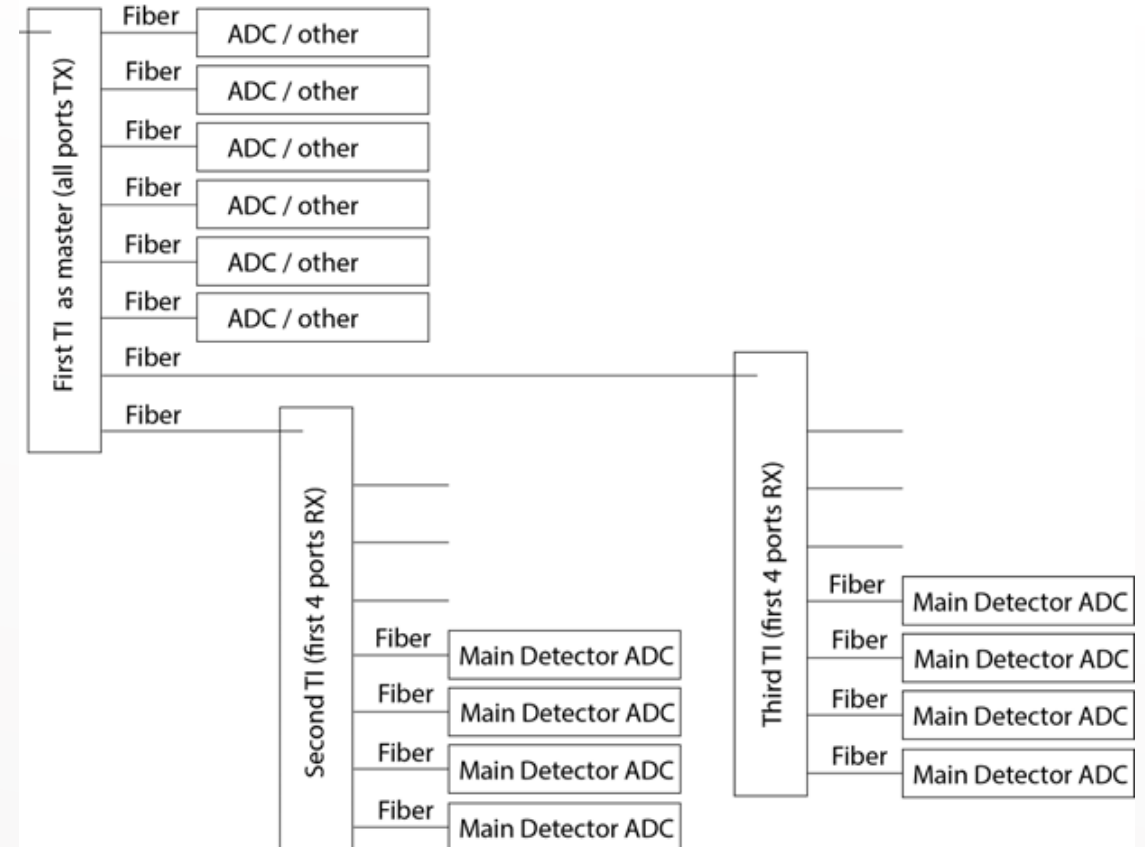


Figure adapted from Malte Wilfert

Integration Mode Front-end Electronics Design (My contribution to P2):

Data acquisition components for integration mode running

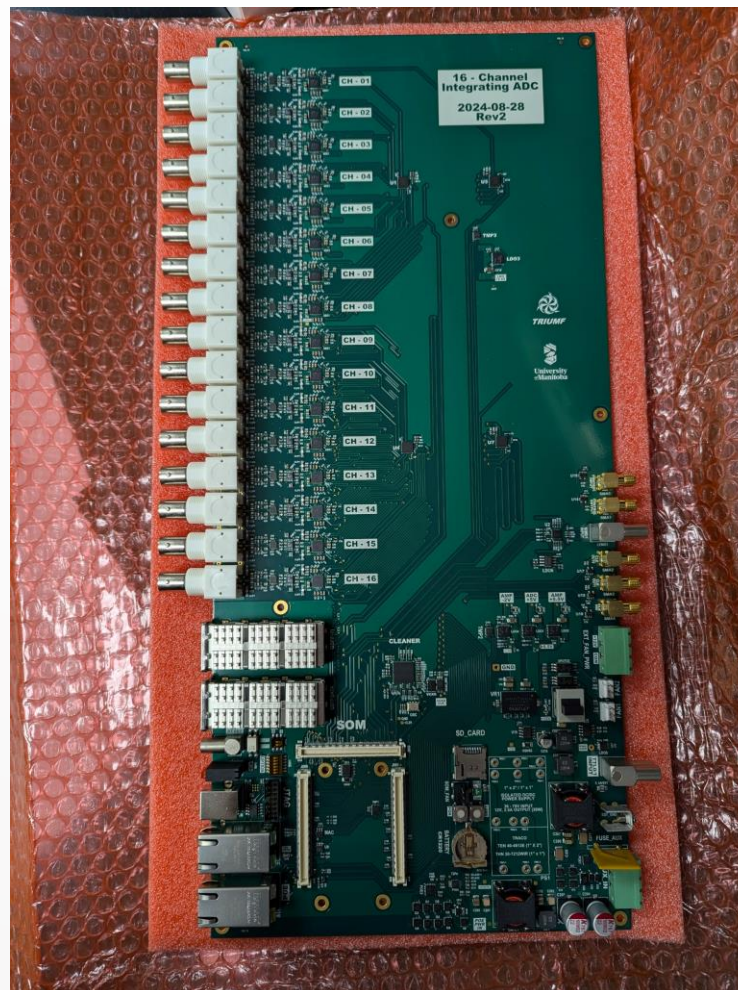
- Two main components:
 - ADC board
 - Trigger interface/distribution
- Each ADC board serves as a trigger slave, receiving clock synchronization, run start, and helicity flip signals
- ADC boards sample and sum signals between helicity triggers and collect timestamp information.
- There will be enough trigger interface ports for all of the main detectors and beam monitors.
- Each ADC board has 16 channels.



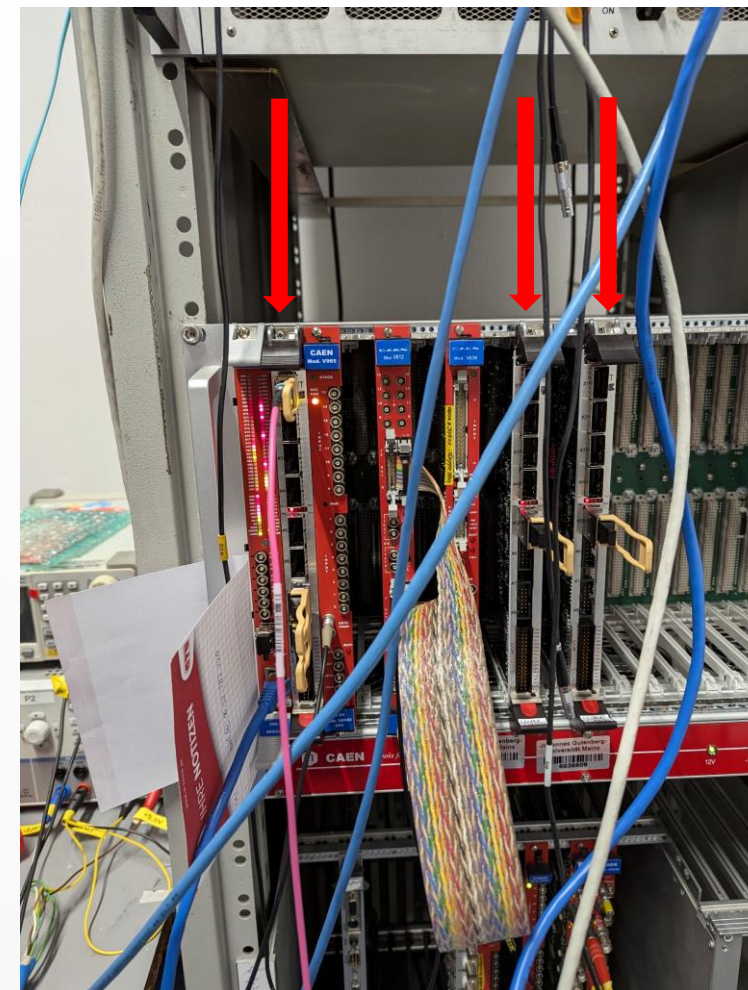
Integration Mode Front-end Electronics Design (My contribution to P2):

Data acquisition components for integration mode running

- Two main components:
 - ADC board
 - Trigger interface/distribution
- The three TI cards needed for P2 are now here (in the P2 counting room)
- The production ADC boards have been received
- Some firmware work remains to be done.



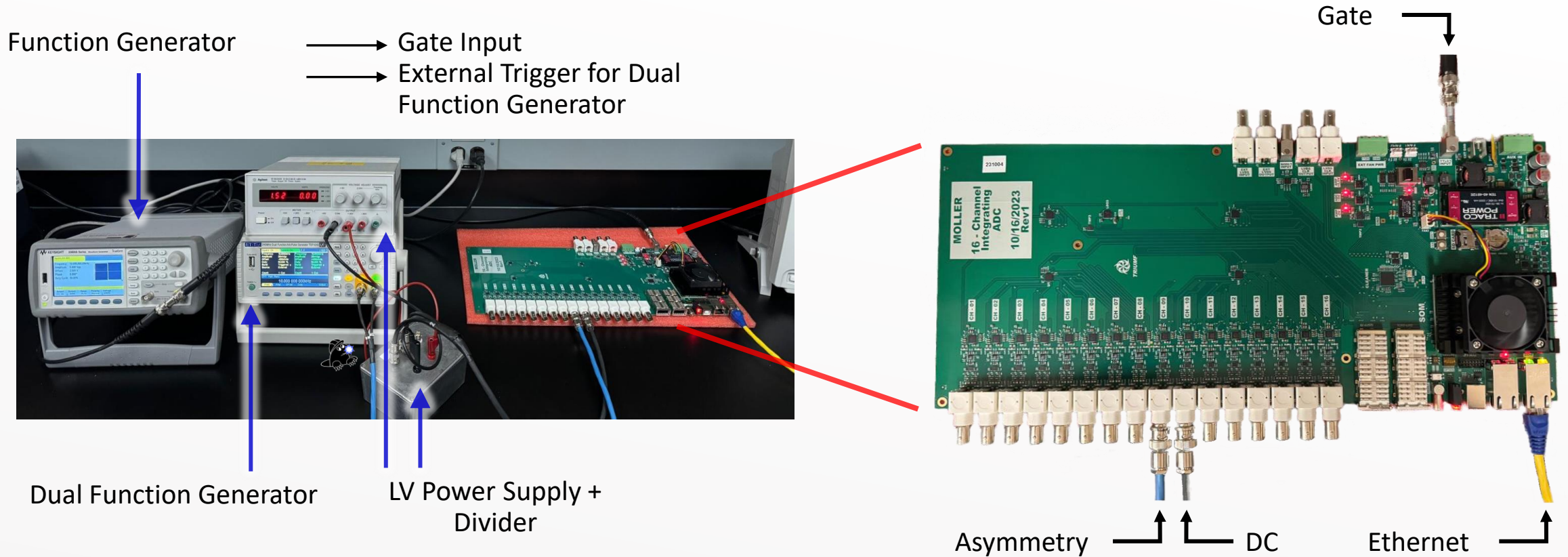
Production ADC Board



Trigger Interface Boards

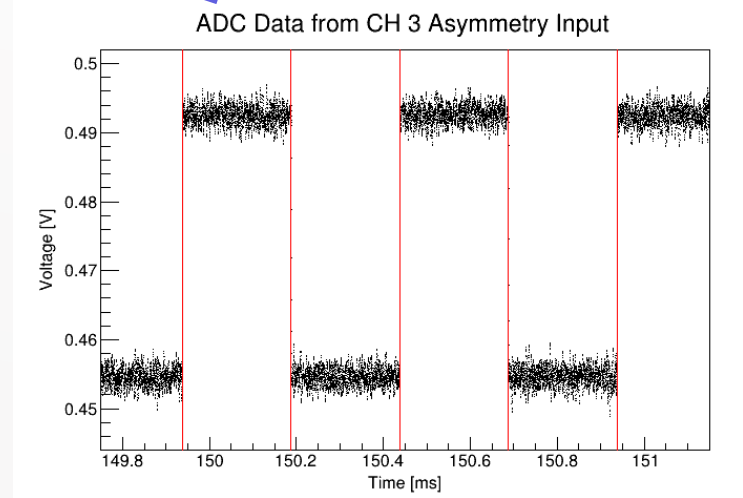
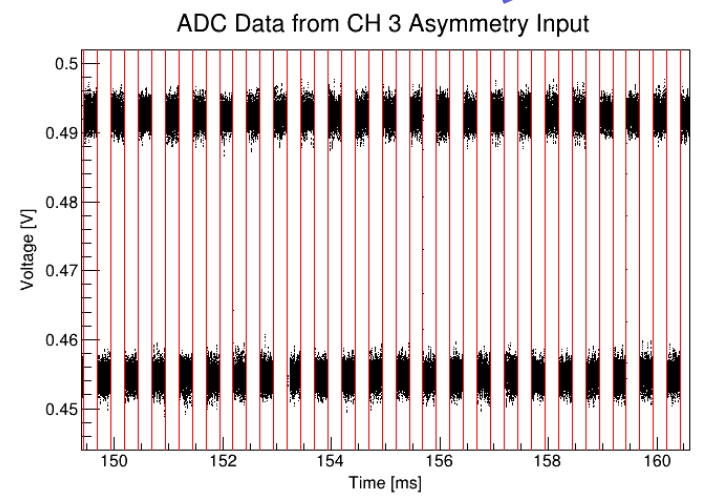
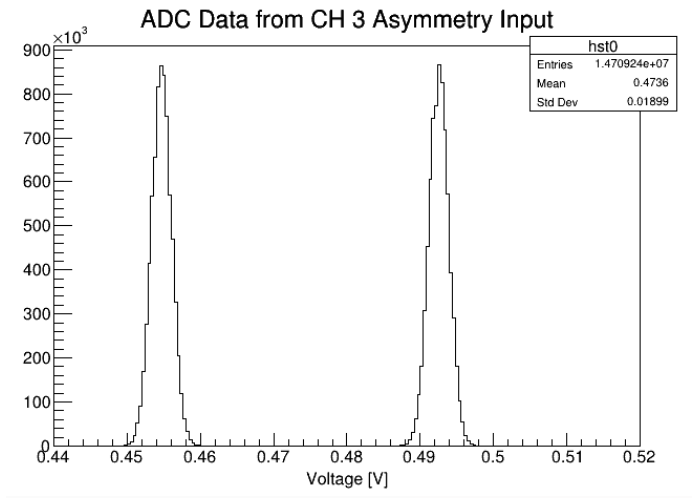
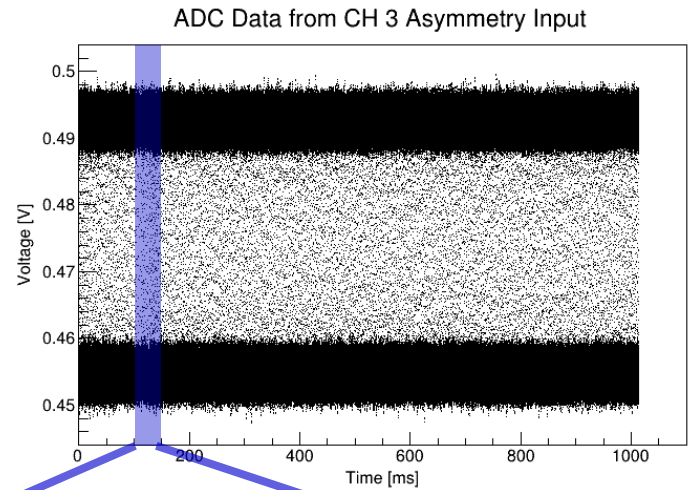
Integration Mode Front-end Electronics Design (My contribution to P2):

ADC board preliminary tests looking for crosstalk between signal inputs on adjacent channels (Brynne Blaikie)



Integration Mode Front-end Electronics Design (My contribution to P2):

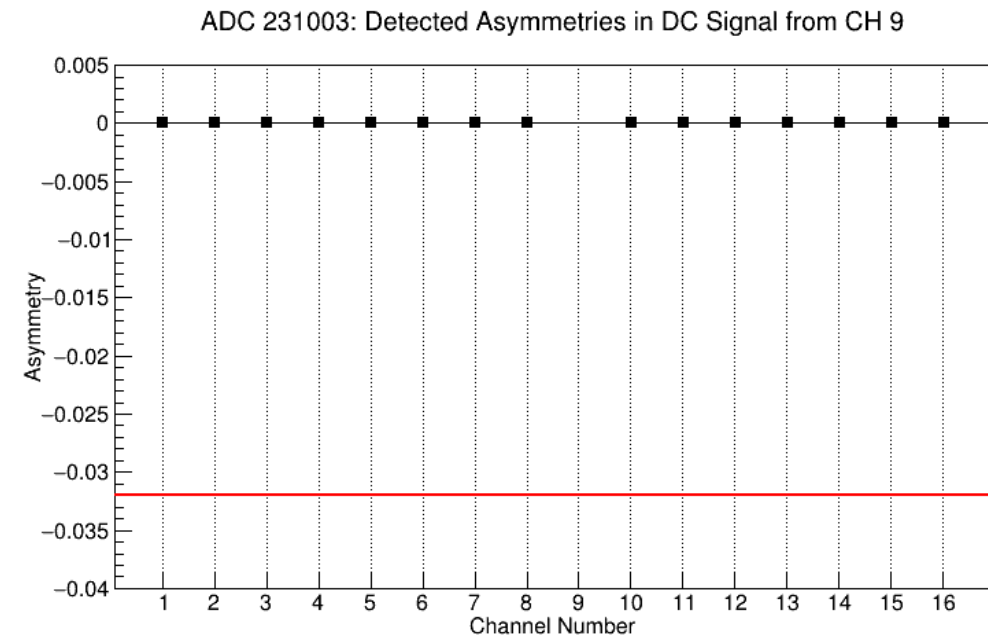
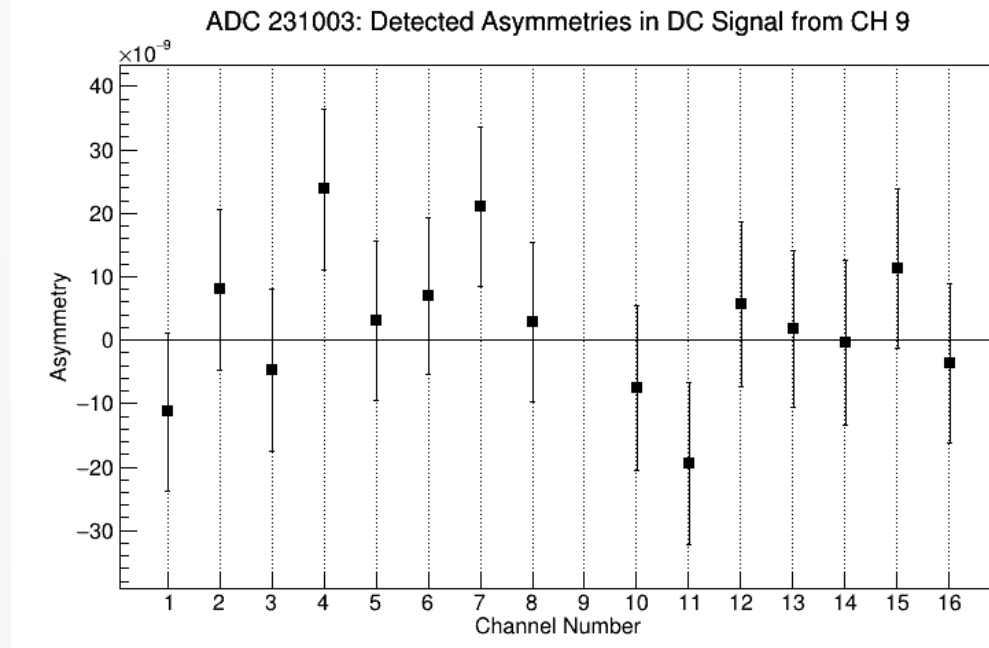
ADC board preliminary tests looking for crosstalk between signal inputs on adjacent channels (Brynnie Blaikie)



ADC board preliminary tests looking for crosstalk between signal inputs on adjacent channels (Brynne Blaikie)

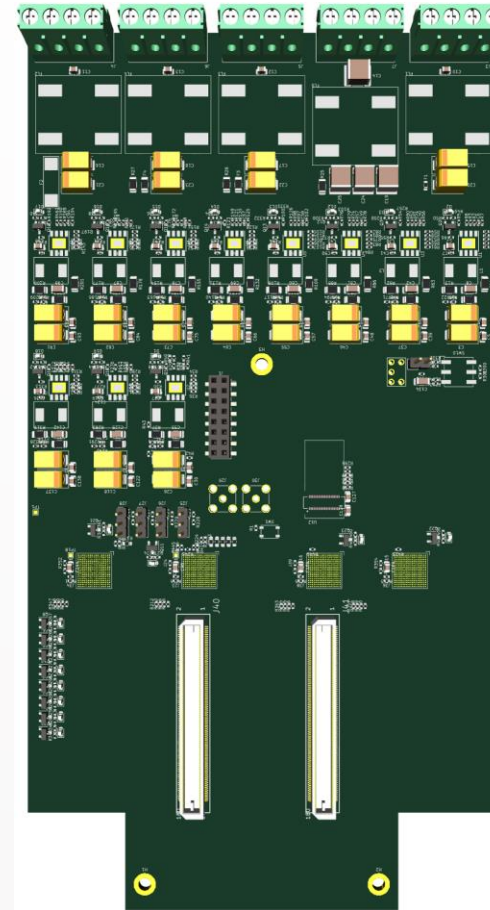
Example:

- 0.032 asymmetry from 10 kHz square wave input, 0.76 V average into Ch. 9
- 0.76 V DC signal for all remaining channels
- 10 x 1 second runs for each channel
- Also demonstrates small time to integrate electronic false asymmetries down to experimental goal precision.



Work on P2 HVMAPS (My contribution to P2):

- Joint production of the P2Pix sensor
 - Funding contribution for engineering run
 - Front-end electronics readout
- Readout board design based on CERN serializer / transceiver chip set – prototype is being assembled
- Some readout board revisions needed for P2Pix
- We are building up capabilities for sensor module assembly – placement, bonding, testing
- We hope to be ready to test P2Pix sensors together with the Mainz group when they arrive next year.
- Plan to contribute to the implementation of the P2 tracking detectors.



Status and Outlook

MOLLER and P2 are roughly on the same trajectory (distressingly ...)

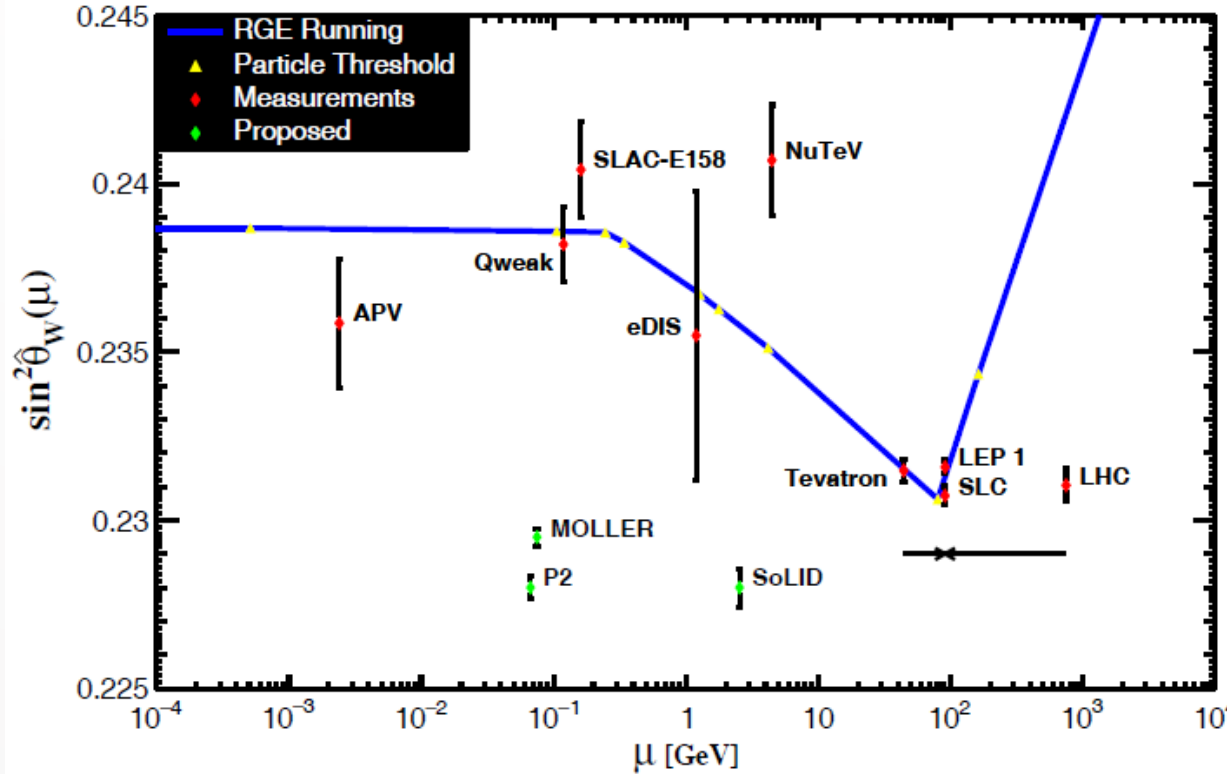
- Both are fully funded
- Both efforts have started with construction of components
- Significant upgrades and new construction underway for Hall A at Jlab
- MESA construction is well advanced
- Installation scheduled to start in late 2025
- Commissioning in 2026
- My contributions on P2 will continue to be on the DAQ and Detector end and migrate to data analysis when we start running.

Thank You!

Backup

The Weak Mixing Angle

J. Erler (JGU), reproduced with permission



The weak mixing angle is a central parameter of the electroweak part of the Standard Model:

$$\begin{pmatrix} \gamma \\ Z^0 \end{pmatrix} = \begin{pmatrix} \sin(\theta_W) & \cos(\theta_W) \\ \cos(\theta_W) & -\sin(\theta_W) \end{pmatrix} \begin{pmatrix} B^0 \\ A \end{pmatrix}$$

SU(2): Gauge fields (B^+, B^-, B^0) and coupling g'

U(1): Gauge field A and coupling g

“On-shell” definition in terms of boson masses:

$$\sin^2(\theta_W) = 1 - \frac{m_W^2}{m_Z^2}$$

“ $\overline{\text{MS}}$ -Scheme” definition in terms of (running) coupling constants:

$$\sin^2(\hat{\theta}_W) = \frac{g'^2}{g^2 + g'^2}$$

PVES Measurements

Measurement Methodology

- Precision scales with event rate (\sqrt{N}) – so the high precision goals require extremely high detector event rates
- Individual detector event counting not always feasible at the highest rates – even with high segmentation and fast electronics
- Integration mode operation of detectors makes sense when:
 - When we deal with high rates, and
 - high segmentation is not an option, and
 - backgrounds can be “eliminated by design”, and
 - technology allows for “low noise operation”
- In this case we measure the integrated detector yield

$$Y_D^\pm \simeq \mathcal{L} \sigma_D G_D (1 \pm PA_{ph} \pm A_{beam} \pm A_{inst}) \pm A_{ped}$$

$$G_D \equiv \Gamma_D Q_{PE} g_{PMT} g_{amp}$$

- Experimental design determines how good this linear approximation will be

PVES Measurements

Measurement Methodology

The faster the helicity reversal the better the approximation of the signal as a linear drift for many experimental effects.

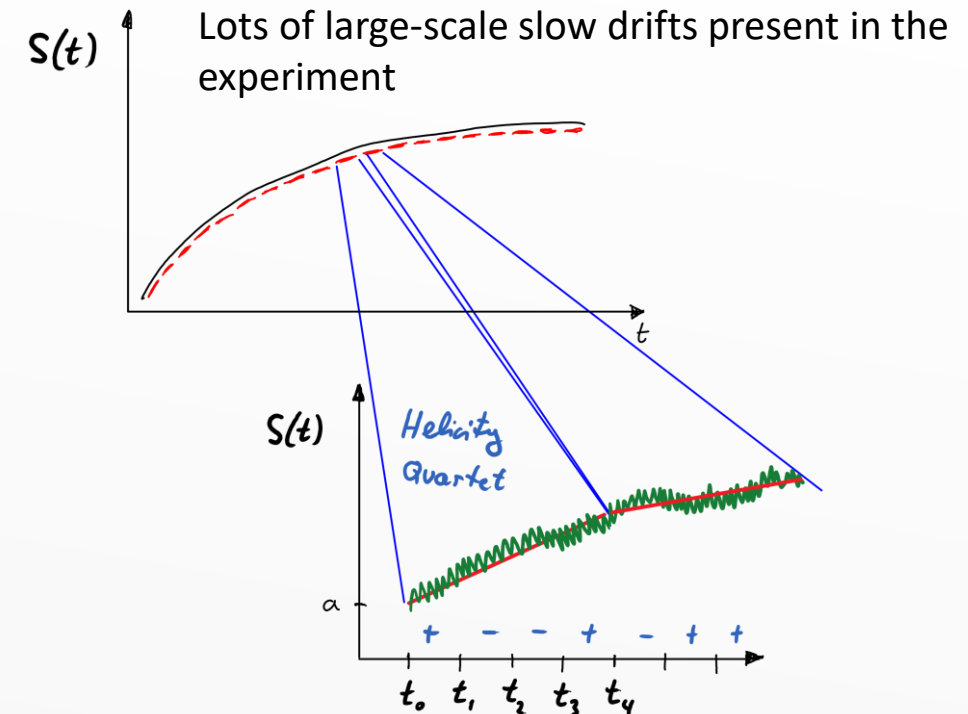
So, locally, the signal “looks like” a linear function of time:

$$Y_{\pm}(t) \approx \left(a + \frac{dY}{dt} \Big|_{t_i} t \right) (1 + A_{msr})$$

- The quartet helicity pattern removes linear drifts +---+ or -++-
- An octet helicity pattern removes quadratic drifts +---+---+
- Pseudo random reversal of the first sign in quartet patterns removes higher order drifts

Example of these drifts:

- Target drifts (e.g. diurnal variations) and boiling noise
- Detector gain and electronics drifts
- Spectrometer field drifts
- Slow beam drifts



Integration Mode Front-end Electronics Design:

$$\text{Detector Yield: } Y^\pm = \mathcal{L}\sigma G^\pm \left(I_c^\pm + \varepsilon(I_c^\pm) \right) + Y_{ped}^\pm$$

$$\text{PMT Cathode Current: } I_c^\pm \equiv \Gamma_C q_{pe} (1 \pm A)$$

$$\text{Detector gain: } G^\pm \equiv g_{PMT} g_{amp}^\pm$$

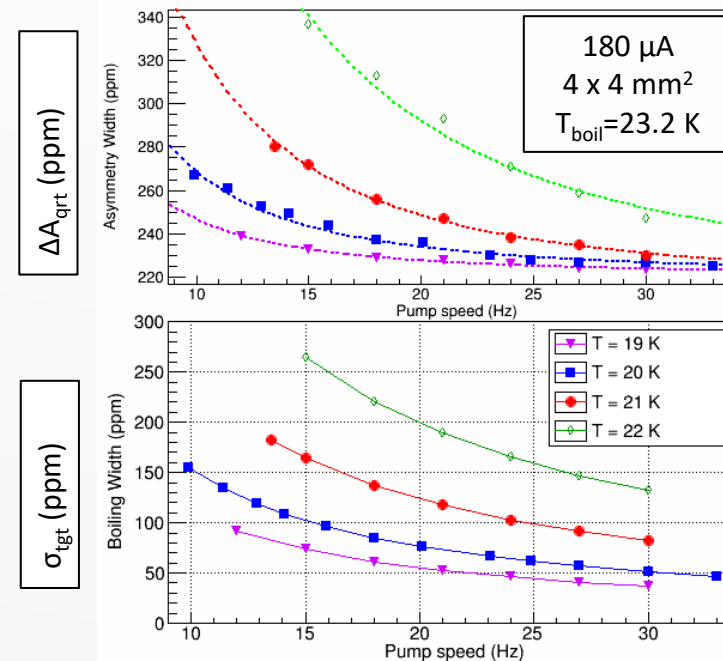
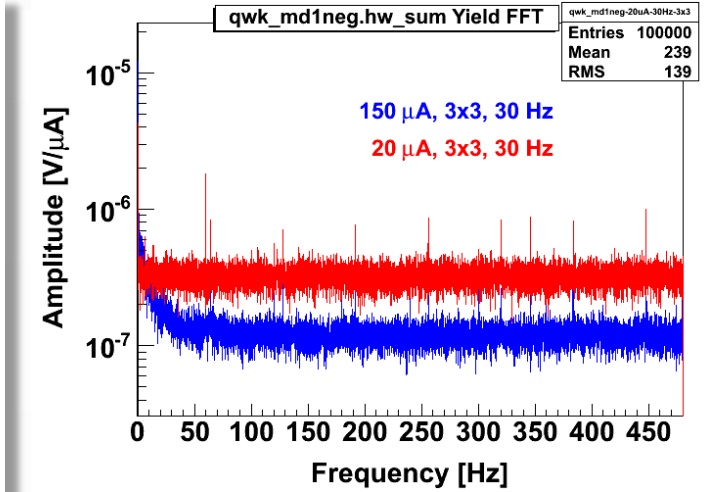
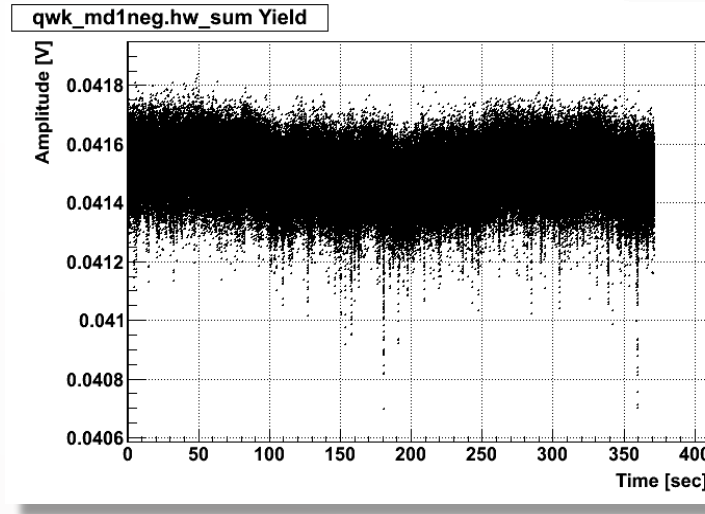
- Light yield (Γ_C): - maximize, based on geometry and materials
- Quantum efficiency (q_{pe}): - UV sensitive, long terms stability, high cathode current
- PMT Gain (g_{PMT}): - low/high gain flexible base design, low noise, good linearity
- Preamp gain (g_{amp}^\pm): - flexible gain, high bandwidth capable, low noise (possibly helicity dependent)
- Non-linearity (ε): - precisely measure PMT non-linearity
- Electronic Pedestal (Y_{ped}^\pm): - keep small and remove/suppress false asymmetries

PVES Measurements

Systematic effect example

Target boiling:

- With high beam power target boiling is inevitable
- Starts around $100 \mu\text{A}$
- Has a $1/f$ frequency dependence
- At low helicity reversal this lead to additional width in the detector and asymmetry signal
- Fast helicity reversal minimizes this effect



PVES Measurements

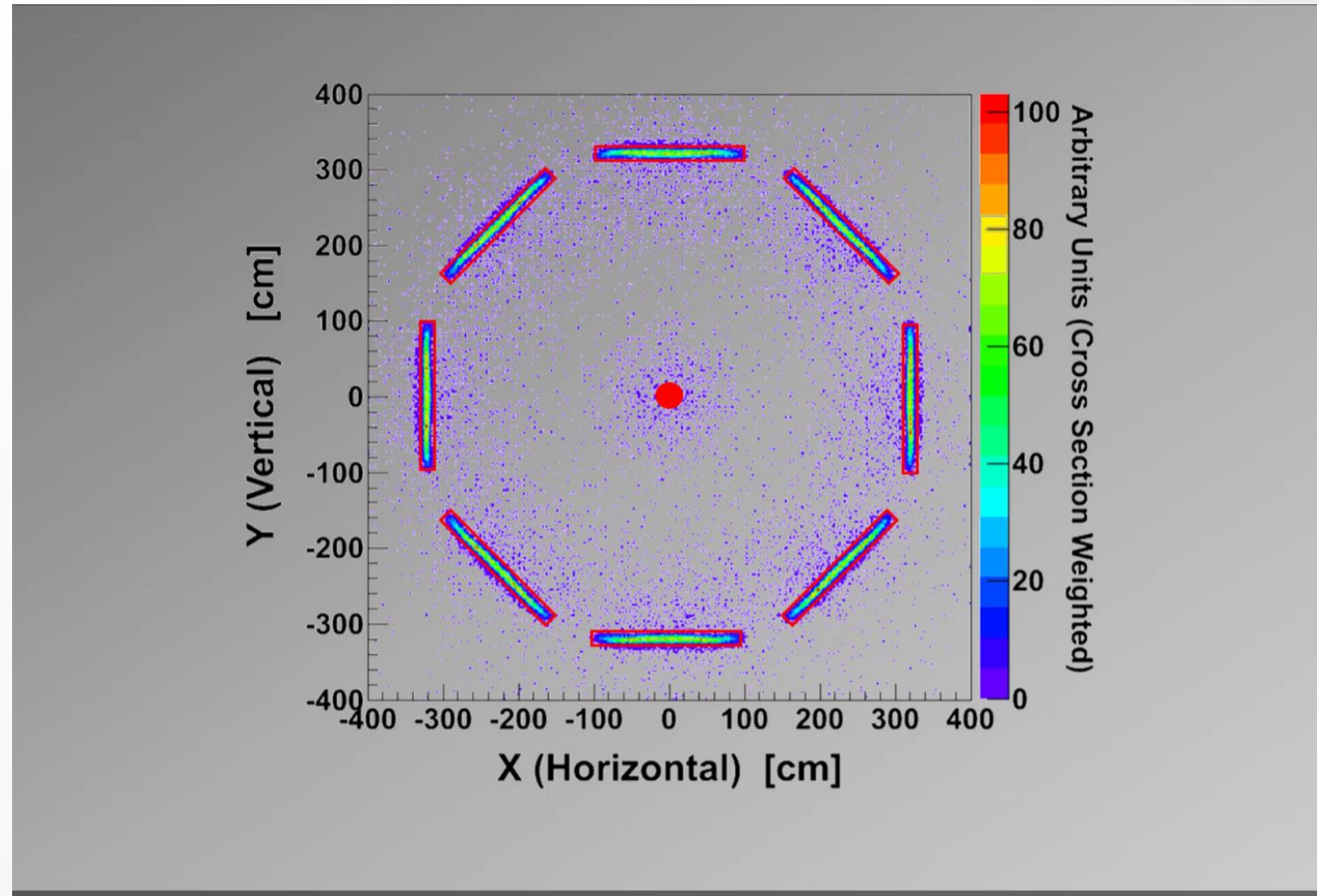
Systematic effect example

Detector symmetry allows measurement of:

- Beam motion
- Beam position
- Beam angle

Performing detector studies that measure the correlation between the detector signal and beam parameters (deliberate variation) is used to remove the corresponding false asymmetries.

Detector symmetry can also be used to measure transverse spin asymmetry.



PVES Measurements

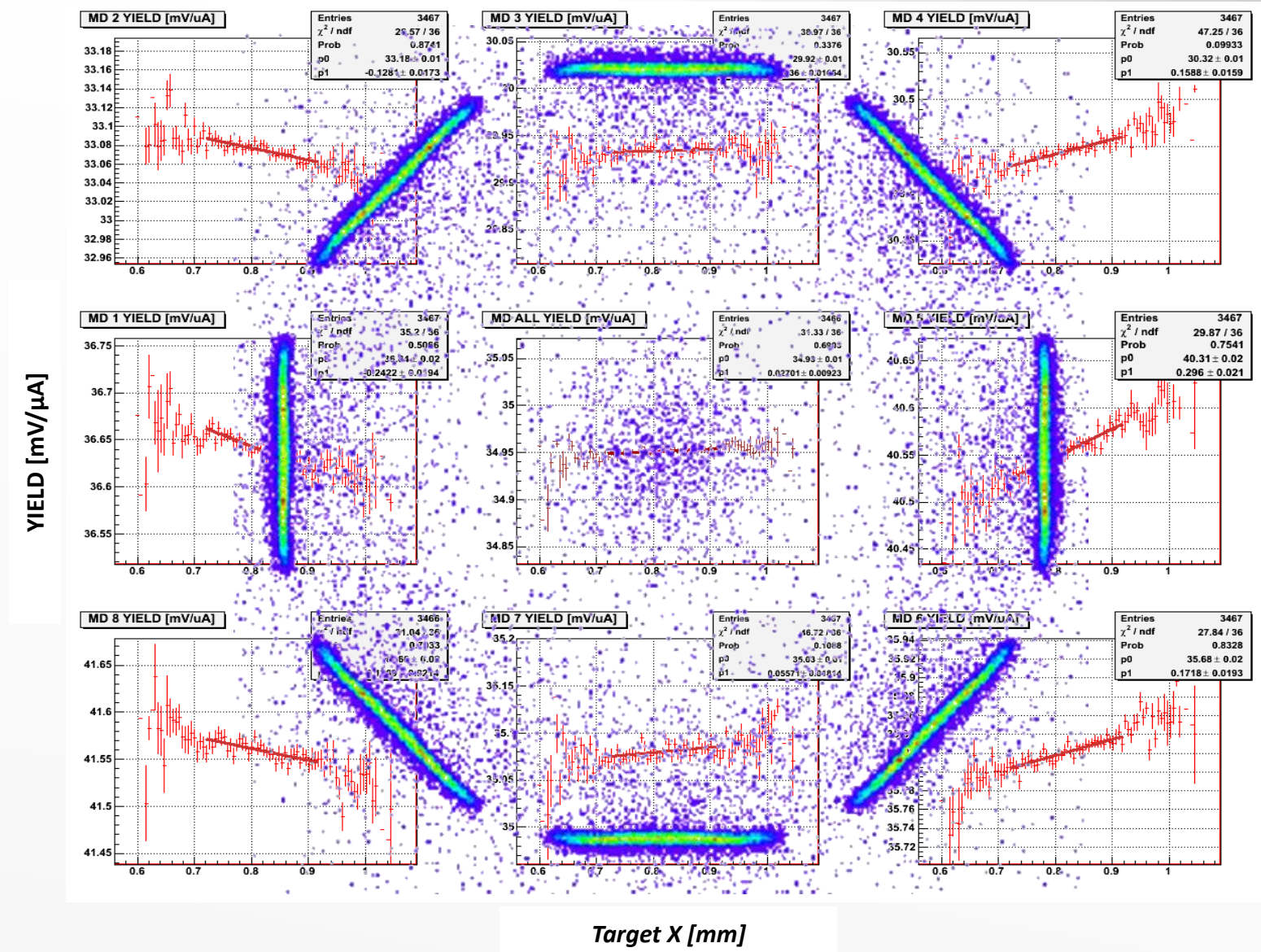
Systematic effect example

Detector symmetry allows measurement of:

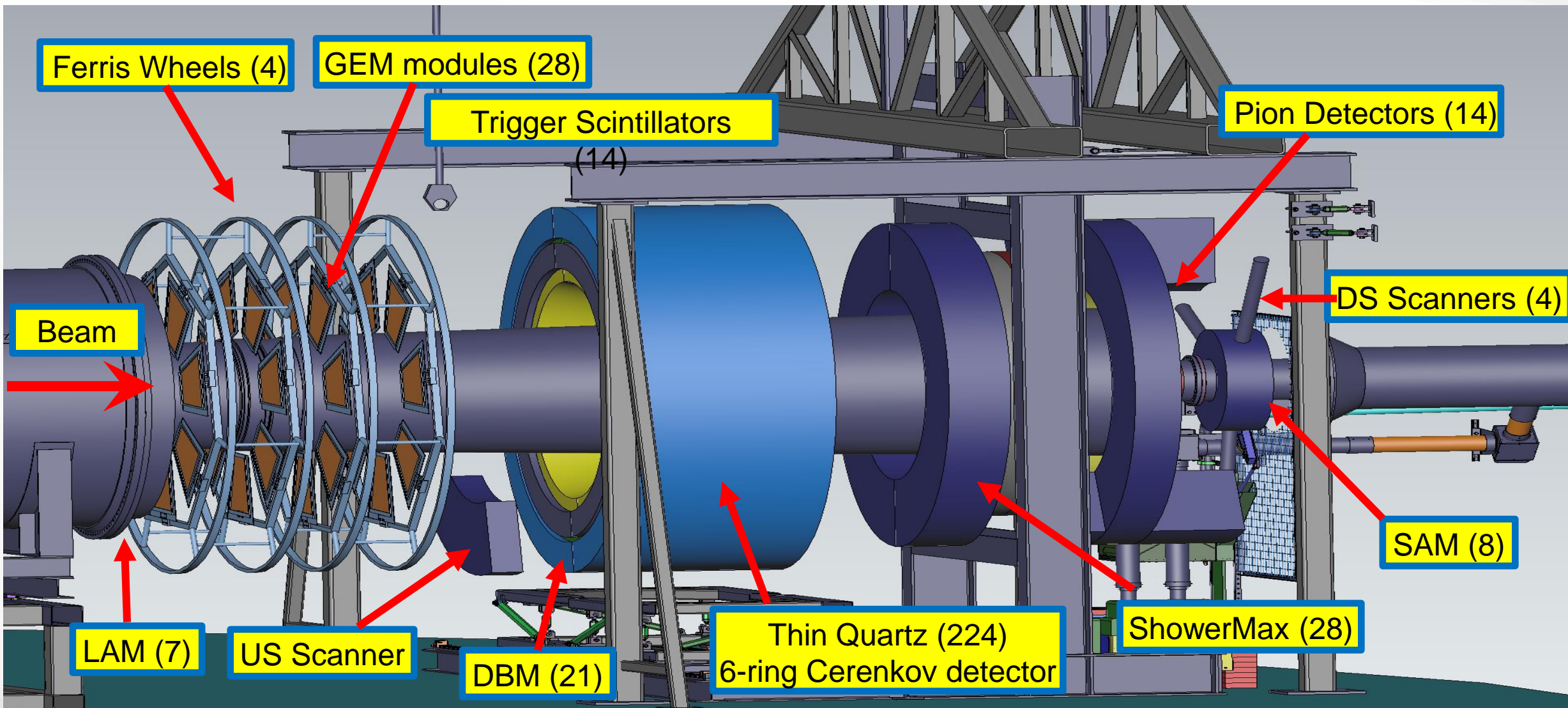
- Beam motion
- Beam position
- Beam angle

Performing detector studies that measure the correlation between the detector signal and beam parameters (deliberate variation) is used to remove the corresponding false asymmetries.

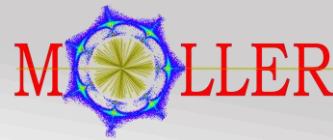
Detector symmetry can also be used to measure transverse spin asymmetry.



MOLLER Experiment



MOLLER Experiment

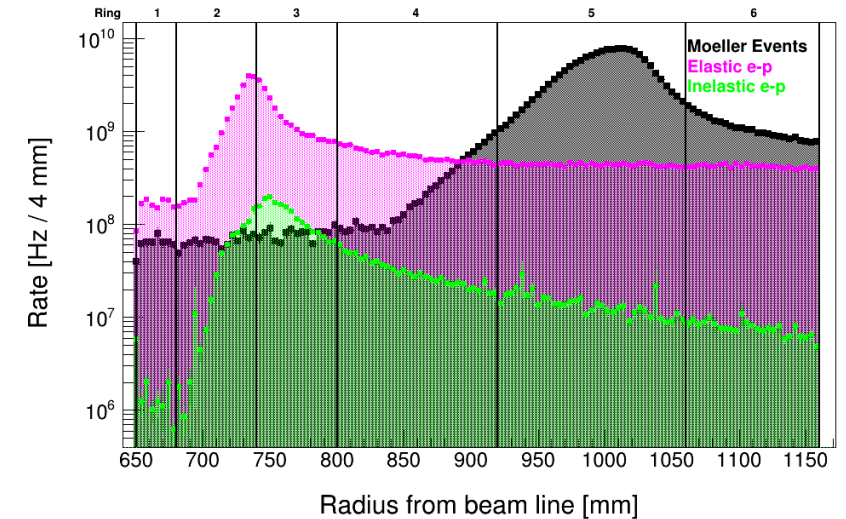
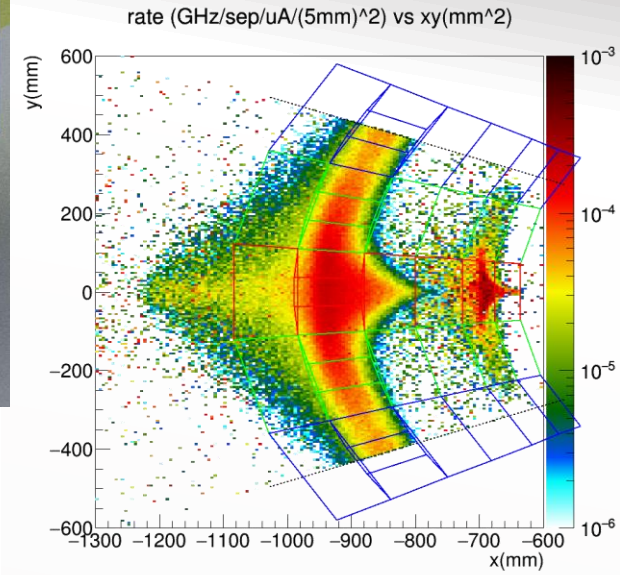
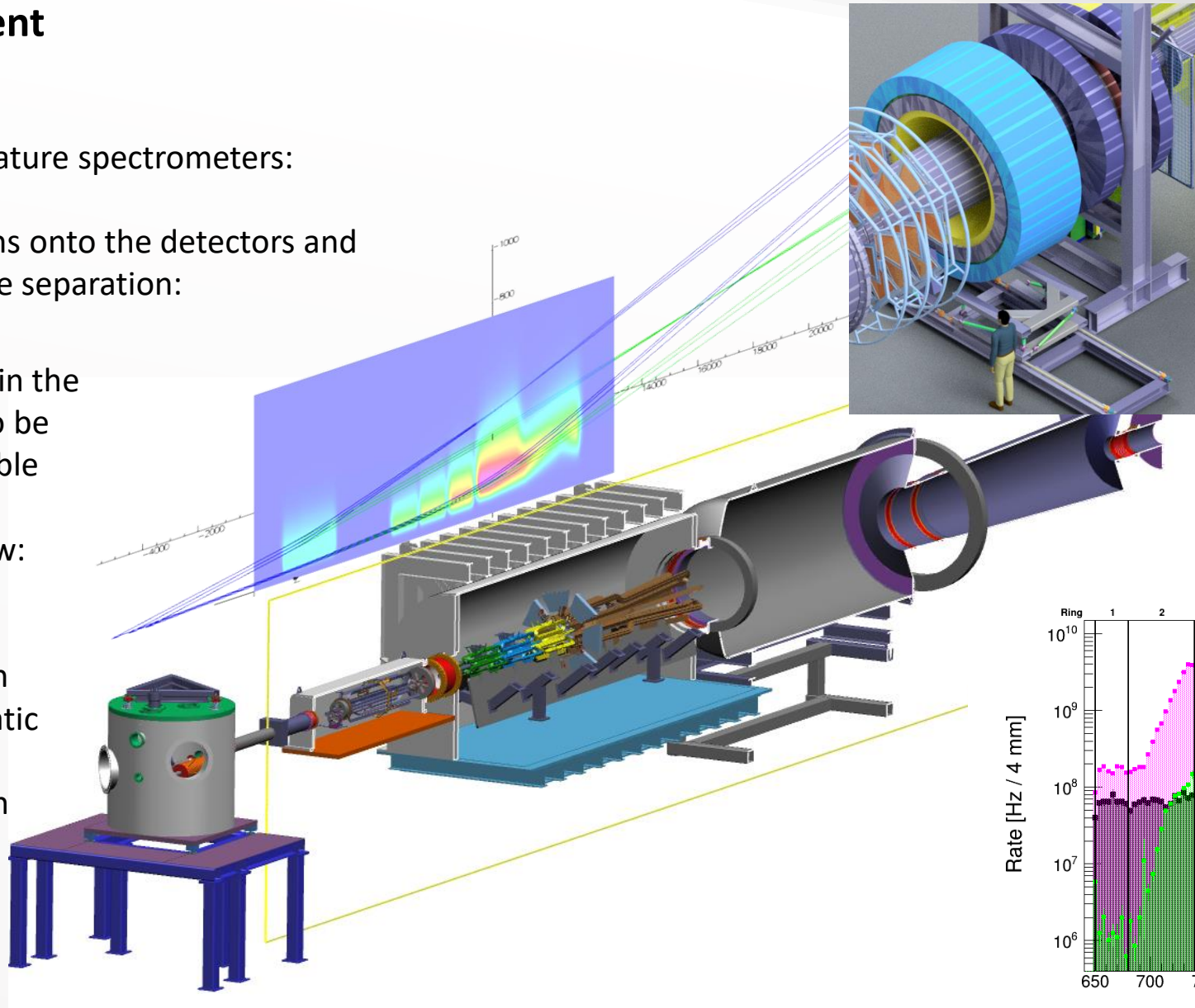


A set of room temperature spectrometers:

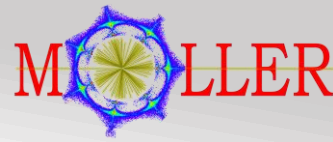
- Steers the electrons onto the detectors and Perform event type separation:

The scattering profile in the detector planes has to be separated into a suitable number of radial and azimuthal bins to allow:

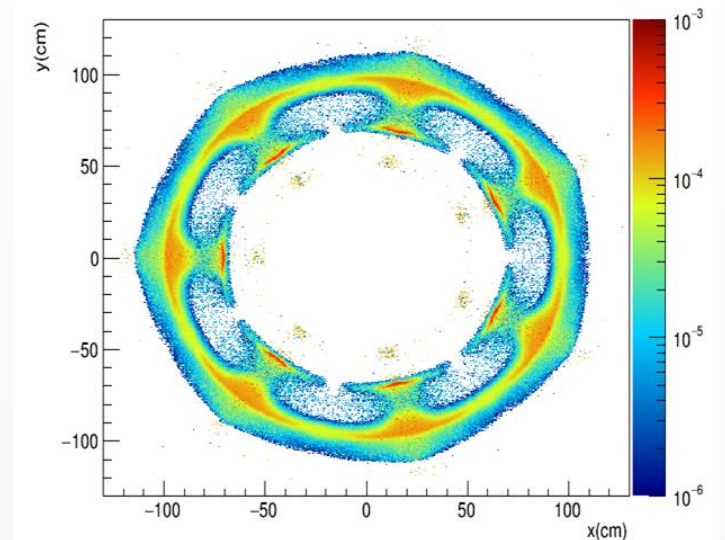
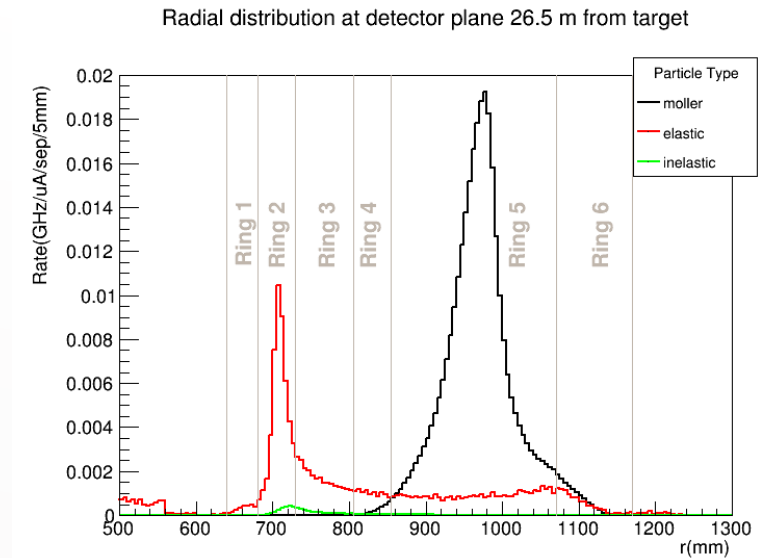
- Event separation,
- Statistics collection
- Control of systematic effects, such
 - Beam motion
 - Backgrounds

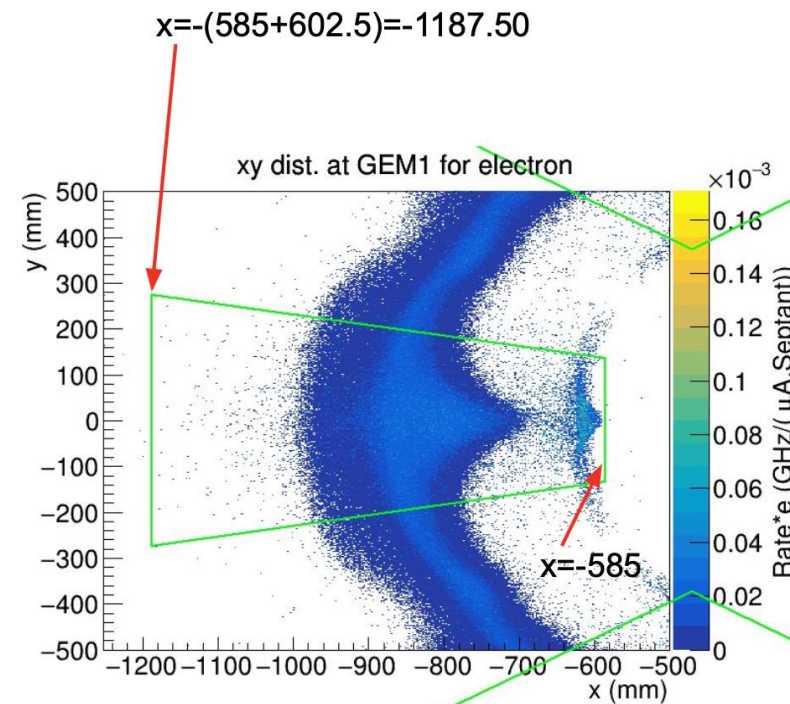
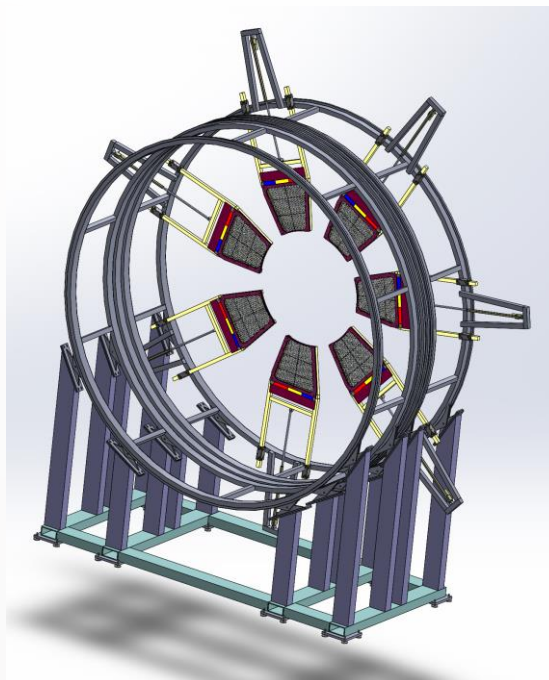
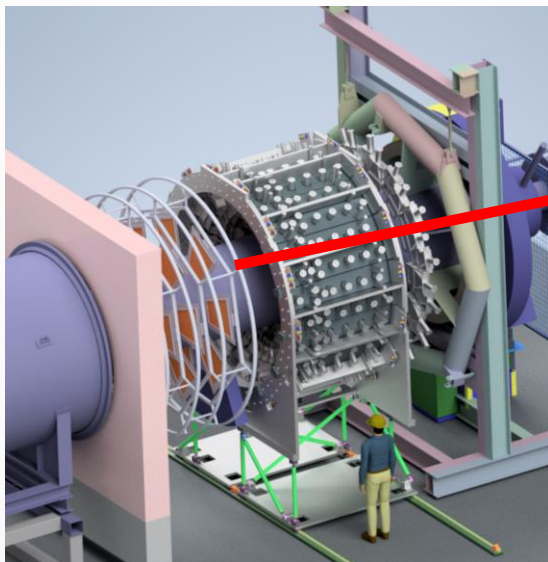


MOLLER Experiment



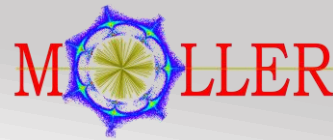
1. Full coverage of $e + e \rightarrow e + e$ events
2. Radial binning to understand backgrounds: $e + p \rightarrow e + p$ and $e + p \rightarrow e + X$
3. Azimuthal binning required for **deconvolution** of $e + e \rightarrow e + e$ from $e + p \rightarrow e + p$ and $e + p \rightarrow e + X$ background
4. Cover wide range of rates across the 224 modules (1 MHz to 4 GHz)
5. Low excess noise
6. Good linearity
7. Suppression of soft backgrounds (photons and neutrons)
8. Radiation hard to peak dose of ~ 35 and ~ 80 Mrad (rings 5 and 2)
9. Suppress false asymmetries





Large area GEM detectors will be used for tracking, together with a set of trigger scintillators.

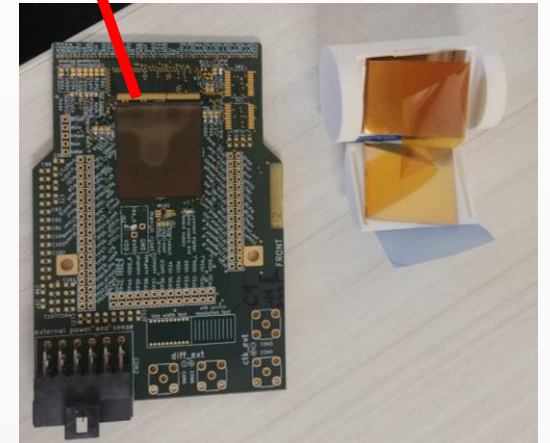
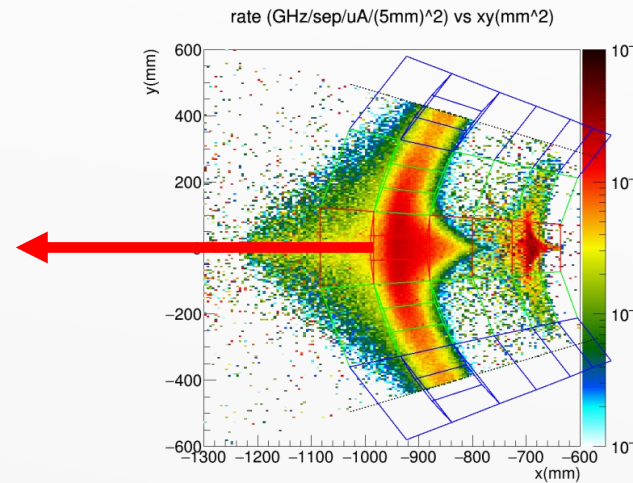
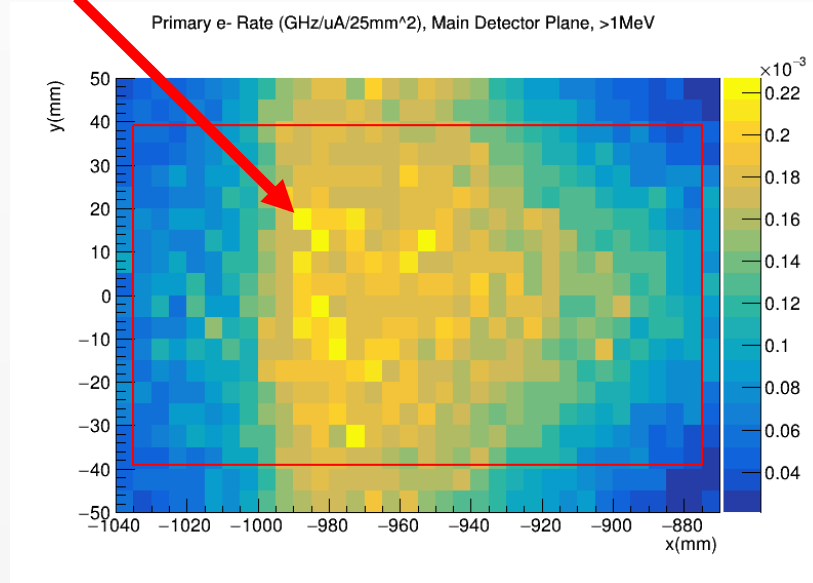
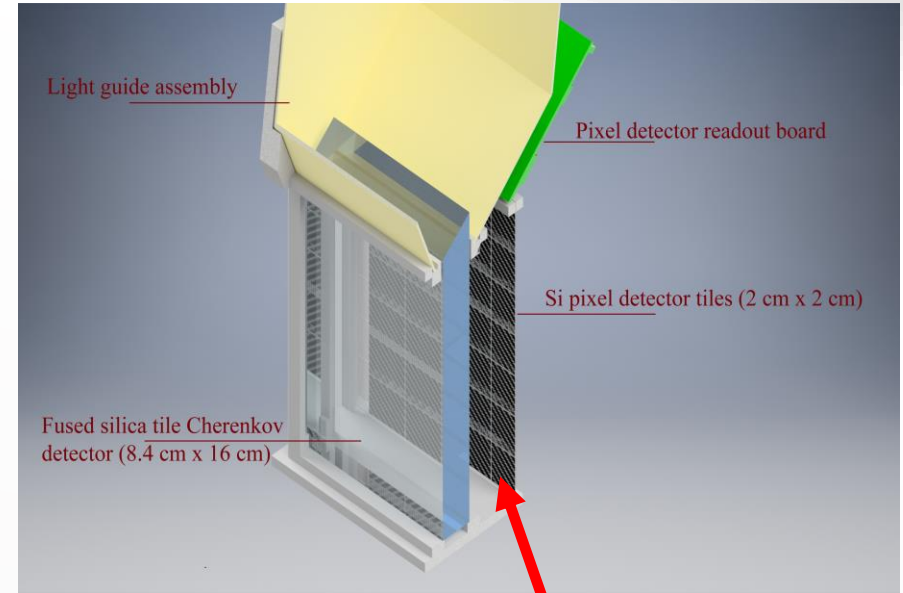
MOLLER Experiment



Ring 5 region includes HVMAPS (same as the P2Pix) to map the scattered profile and to be used in tracking mode to diagnose detector performance. This includes

1. Chips (estimate 80 wavers, with 40 chips each)
2. Mounting structure (including flex-print)
3. Readout boards (84, one for each detector)
4. FPGA boards

$$R = 2.2 \times 10^{-4} \times 70/25 \approx 600 \text{ kHz/mm}^2 \Rightarrow \approx 4 \text{ kHz/pixel}$$

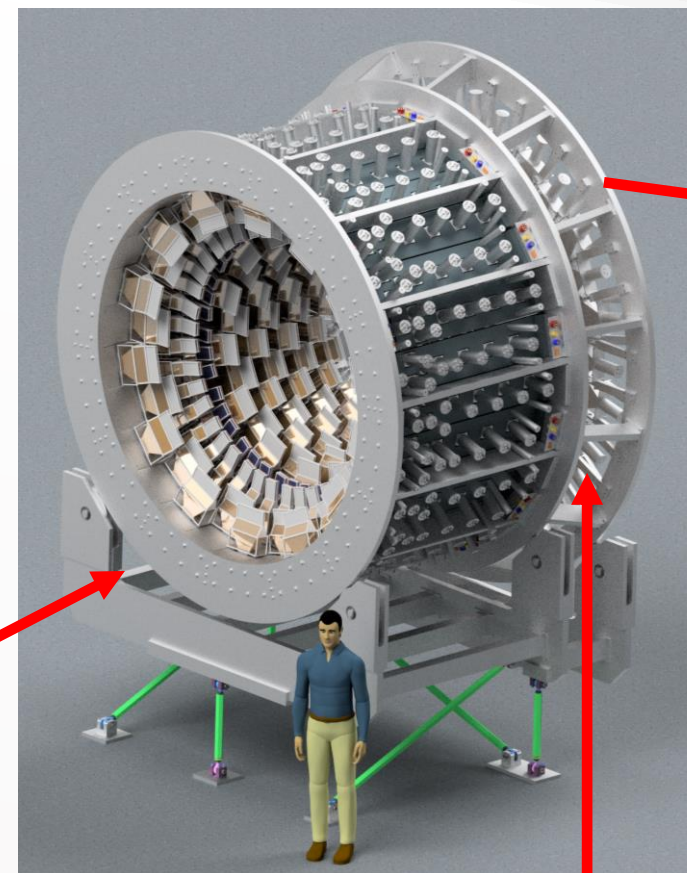
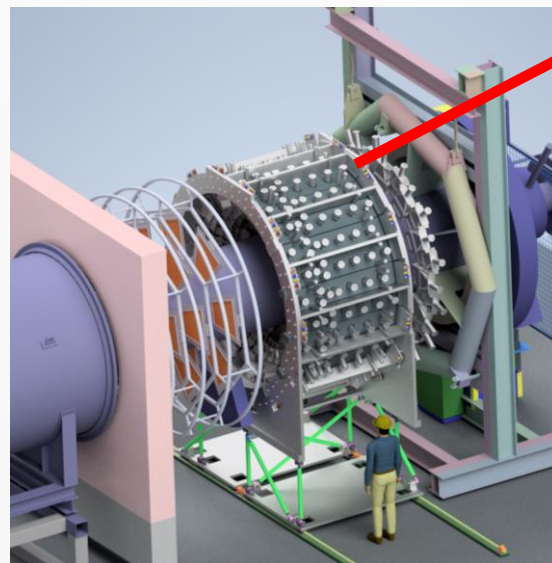


MOLLER Experiment

There are an additional 28 shower max sandwich detector modules including

1. Mounting structure
2. Quartz active material
3. Tungsten radiator material
4. Light guide
5. Photo-multiplier tube and base
6. Preamplifier
7. ADC
8. Cabling, Power Supplies, etc.
9. Cooling/dry air flushing

These are designed to make and energy weighted asymmetry measurement of the elastic Moeller peak are less sensitive to soft background.



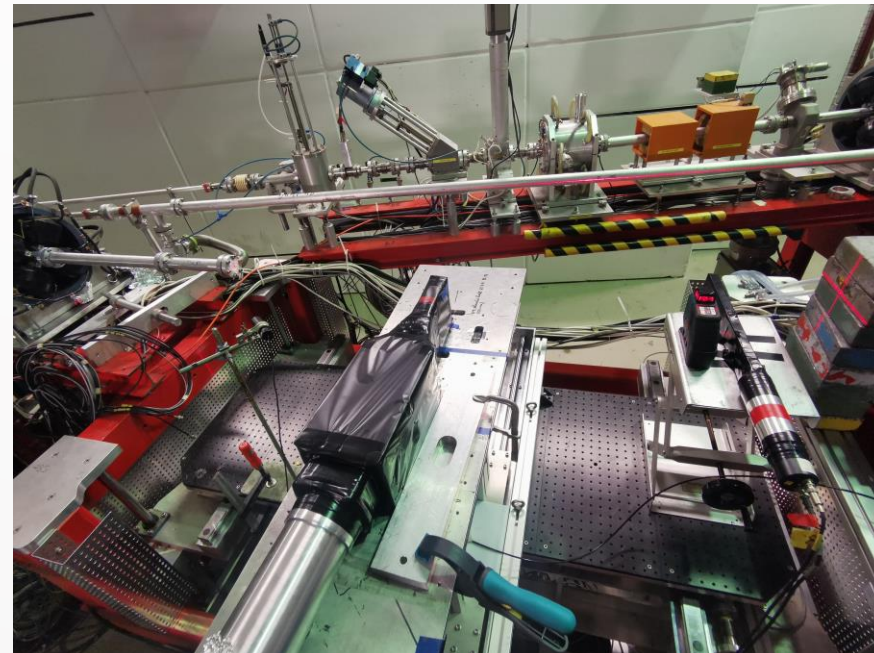
28 Shower Max Sandwich detector behind Ring 5



Detector Prototype Tests:

May 2022 beam time:

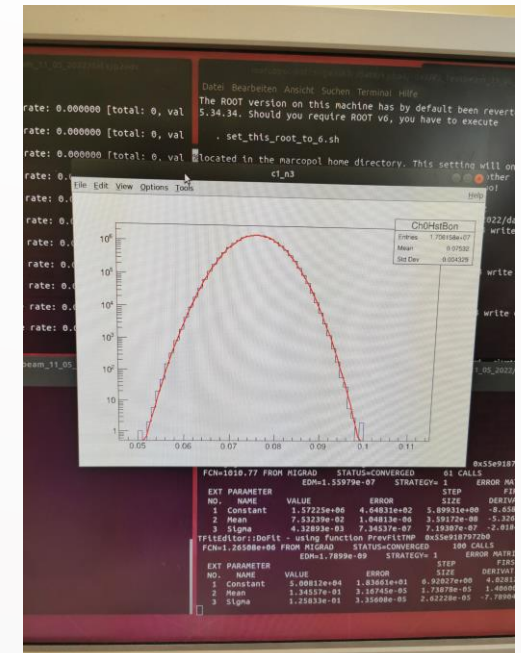
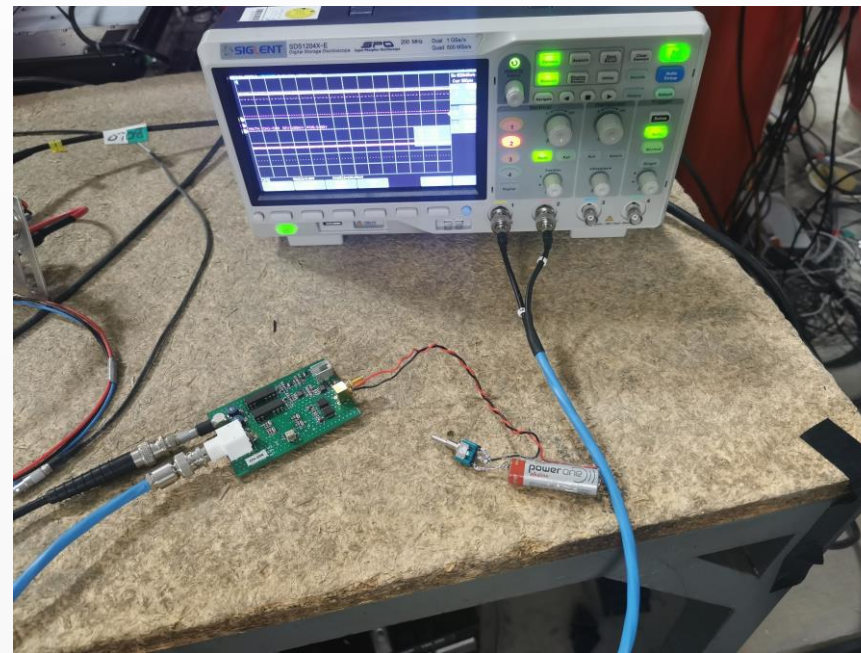
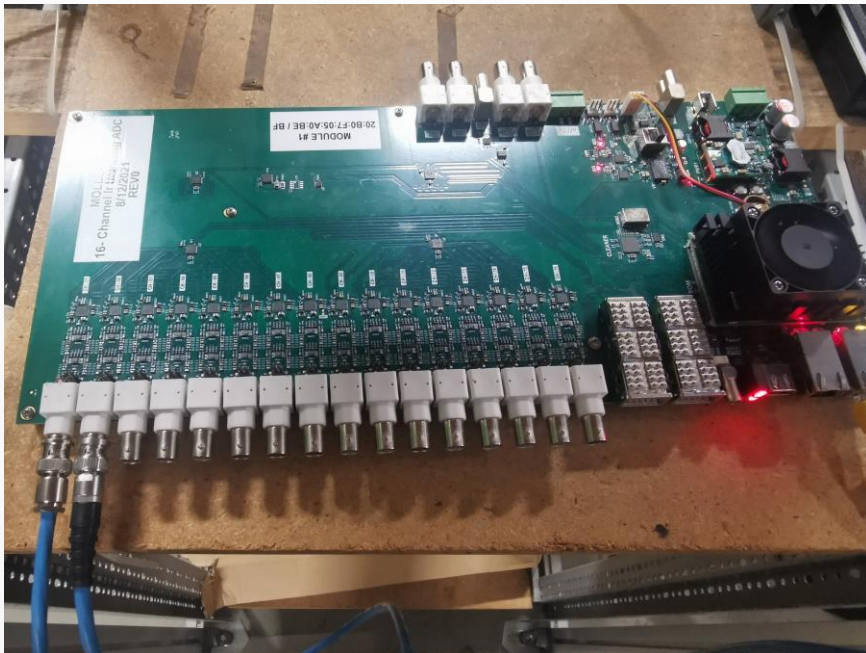
- The PMT/electronics housing is a combination of 3D printed holder and aluminum housing (the top part would be metal as well in the final design)
- The PMT/electronics holder inserts into housing and is held by bayonet twist



Electronics Development:

May 2022 beam time:

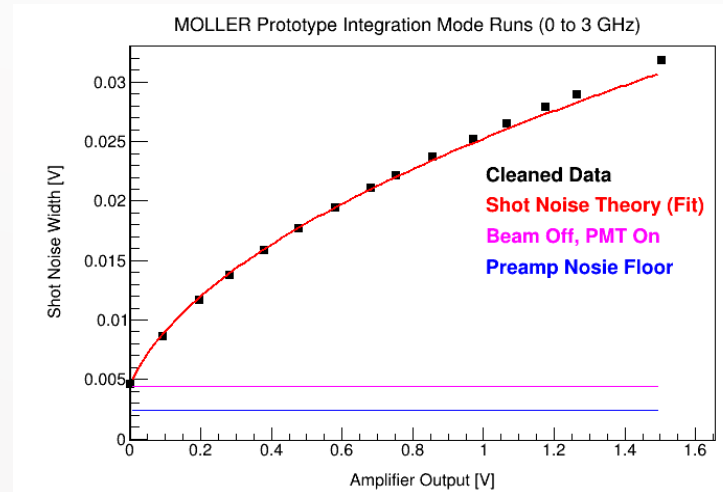
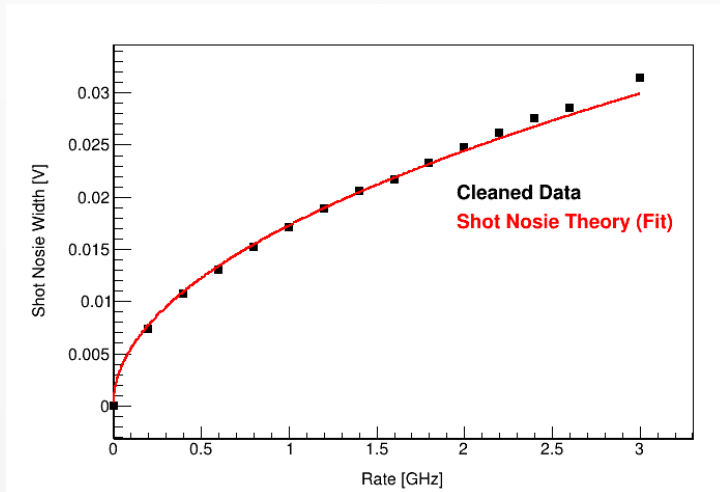
- Custom low noise 16 channel ADC board (developed at U Manitoba and TRIUMF)
- Beam test was conducted with full integrating electronics chain including first full 16 channel ADC board



Detector Prototype Tests:

May 2022 beam time:

- Tested various detector module geometries with different light guide materials and quartz thickness
- Tested the full integrating (with the two-channel prototype board) and event mode electronics chain
- Most important integration mode test is counting statistics performance at high beam current (see plots below) – tests showed excellent performance of the prototype



Appendix

Detector Yield: $Y^\pm = \mathcal{L}\sigma G^\pm \left(I_c^\pm + \varepsilon(I_c^\pm) \right) + Y_{ped}^\pm$

PMT Cathode Current: $I_c^\pm \equiv \Gamma_C q_{pe} (1 \pm A)$

Detector gain: $G^\pm \equiv g_{PMT} g_{amp}^\pm$

- Light yield (Γ_C): - maximize, based on geometry and materials
- Quantum efficiency (q_{pe}): - UV sensitive, long terms stability, high cathode current
- PMT Gain (g_{PMT}): - low/high gain flexible base design, low noise, good linearity
- Preamp gain (g_{amp}^\pm): - flexible gain, high bandwidth capable, low noise (possibly helicity dependent)
- Non-linearity (ε): - precisely measure PMT non-linearity
- Electronic Pedestal (Y_{ped}^\pm): - keep small and remove/suppress false asymmetries

Appendix

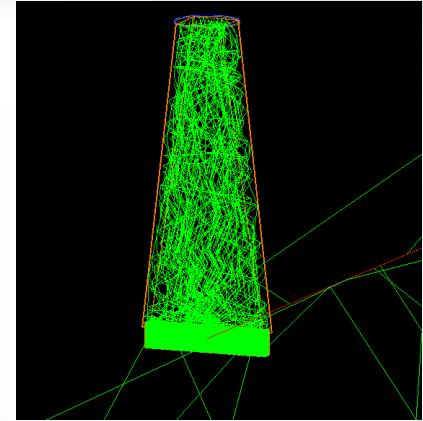
- Light yield (Γ_c):

Light yield depends on quartz thickness, purity, geometry, and surface quality

Light readout depends on light guide material and geometry

The design is based on extensive simulations verified and benchmarked with test beam data

The Cherenkov light emitted from the quartz is primarily in the UV



- Quantum efficiency (q_{pe}):

The PMT was chosen to satisfy a high QE in the UV (with quartz window)

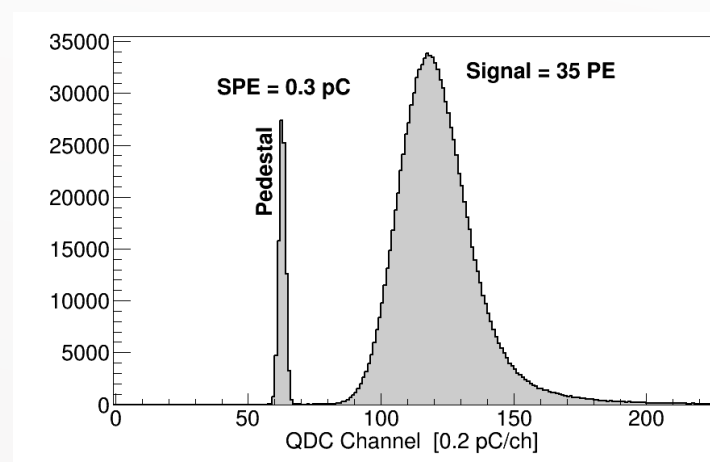
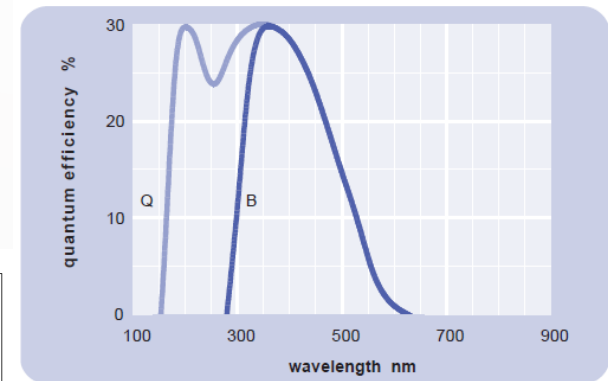
Goal is to maximize the number of photoelectrons

Current model was used in all beam tests

Combined detector geometry and PMT give:

$$n_{pe}(r) \simeq 35 \quad \text{Ring 5 (Møller)}$$

$$n_{pe}(r1) \simeq 16 \quad \text{Ring 1 (Longest light guide)}$$



Appendix

- PMT currents (I_{cath}^{\pm})

Need to keep cathode and anode currents around $10 - 20 \text{ nA}$ and $10 \text{ }\mu\text{A}$ respectively

Maximum PMT currents are 500 nA and $100 \text{ }\mu\text{A}$ respectively (for the selected model)

Ring 5: The 35 n_{pe} and $R = 4 \text{ GHz}$ gives $I_c^{\pm} \simeq 22 \text{ nA}$ so the gain should be about $g_{PMT} \simeq 500$

- PMT gain (g_{PMT})

Definition of PMT end-of-life: g_{PMT} dropped by factor of 2

Reached at about $\simeq 300 \text{ C}$ for a $10 \text{ }\mu\text{A}$ anode current (1 year)

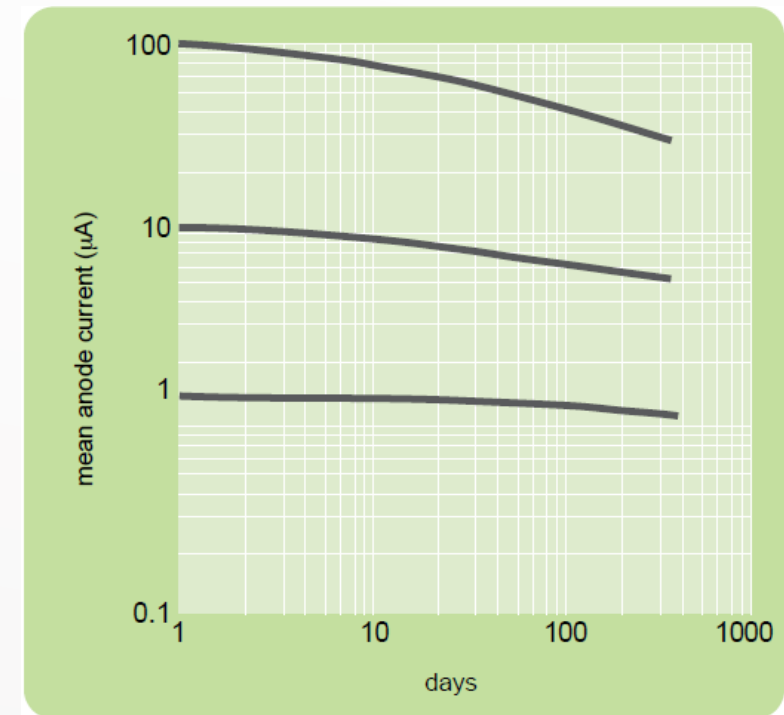
Have few dynodes with high gain on each to reduce excess noise non-linearity

- PMT non-linearity (ε)

PMT Non-linearity produces a false asymmetry: $\varepsilon(I_{cath}^{\pm}) = \sum_{n=2}^N \alpha_n (I_{cath}^{\pm})^n$

$$A_{meas} = A_{Ph} \left(1 + \frac{\sum_{n=2}^N (n-1) \alpha_n (I_c)^n}{I_c + \sum_{n=2}^N \alpha_n (I_c)^n} \right) = A_{Ph} + A_{False}$$

Want to suppress the non-linearity to $\varepsilon \leq 0.5 \pm 0.1 \%$



Appendix

- Excess noise $\left(\frac{1}{\sqrt{N}}\sqrt{1 + \alpha_{exc}^2}\right)$

Need to keep noise contributions above counting statistics to: $\sqrt{1 + \delta_{Det}^2 + \delta_{PMT}^2 + \delta_{Elect}^2} - 1 \leq 4\%$

$$\frac{\sigma_a}{I_a} = \frac{1}{\sqrt{N}} \sqrt{1 + \frac{\sigma_{n_{pe}}^2}{\langle n_{pe} \rangle^2} + \frac{1}{\langle n_{pe} \rangle \delta_{d1}} \left(1 + \frac{1}{\delta_{d2}} + \frac{1}{\delta_{d2} \delta_{d3}}\right)} = \frac{1}{\sqrt{N}} \sqrt{1 + \frac{\sigma_{n_{pe}}^2}{\langle n_{pe} \rangle^2} + \delta_{PMT}^2}$$

Largest contribution comes from detector resolution: $\frac{\sigma_{n_{pe}}^2}{\langle n_{pe} \rangle^2} \leq 6.25\%$ (for $n_{pe} = 16$)

PMT noise depends on base design. The goal is: $\delta_{PMT}^2 < 1\%$ (see backup slides for an example)

Electronics noise (largely DAQ and Trigger WBS): $\delta_{Elect}^2 < 1\%$ ($\delta_{Elect}^2 = 4k_B TR + \delta_{Amp}^2 + \delta_{ADC}^2$)

Electronics and noise behavior is well understood / under control, based on previous work (e.g. Qweak, PREX, etc.)

Appendix

PMT Design:

Three stage PMT ($n = 3$):

Excess noise:
$$\frac{\sigma_a}{I_a} = \frac{1}{\sqrt{N}} \sqrt{1 + \frac{\sigma_{n_{pe}}^2}{\langle n_{pe} \rangle^2} + \frac{1}{\langle n_{pe} \rangle \delta_{d1}} \left(1 + \frac{1}{\delta_{d2}} + \frac{1}{\delta_{d2} \delta_{d3}} \right)} = \frac{1}{\sqrt{N}} \sqrt{1 + \frac{\sigma_{n_{pe}}^2}{\langle n_{pe} \rangle^2} + \alpha_{PMT}^2}$$

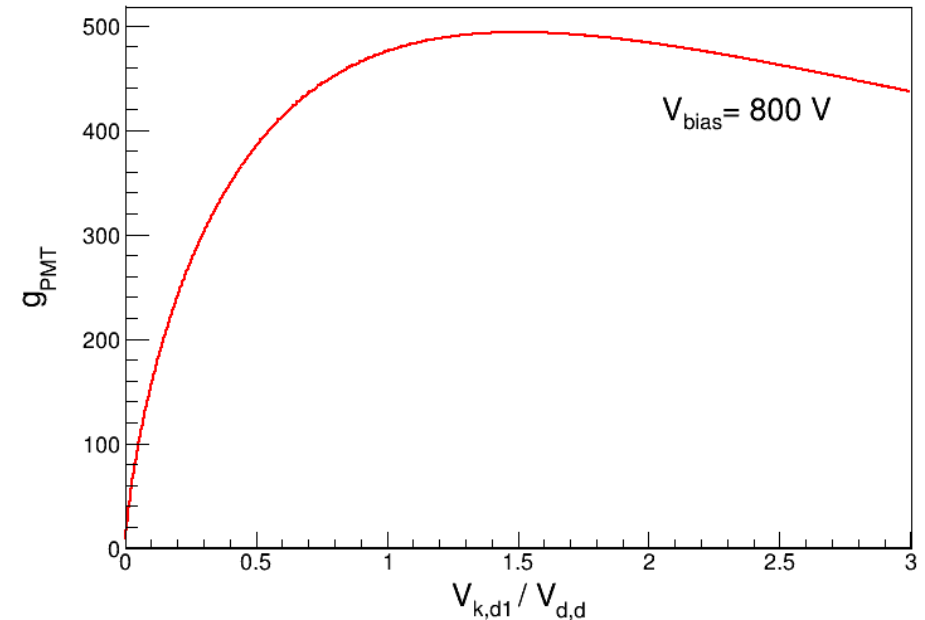
Gain:
$$g_{PMT} = a V_{k,d1}^b (a V_{d,d}^b)^{n-1}$$

For *SbCs* dynodes $a = 0.172$, $b = 0.72$

We'd have

$$\begin{aligned} V_{k,d1} &= 267 \text{ V} \\ V_{d,d} &= 178 \text{ V} \\ \delta_{d1} &= 9.6 \\ \delta_{d2} = \delta_{d3} &= 7.2 \\ G &\simeq 500 \end{aligned}$$

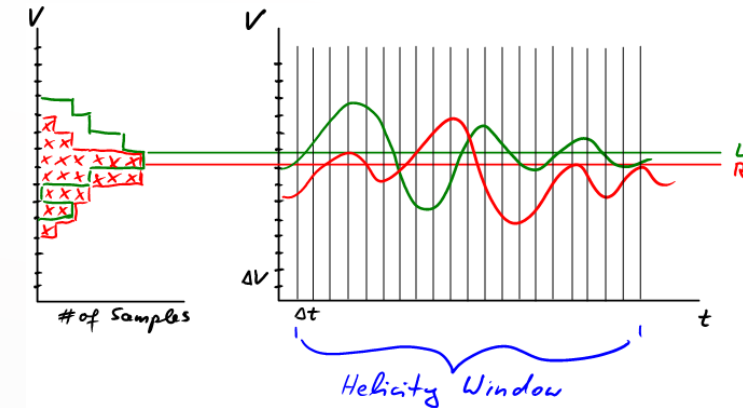
So for $\langle n_{pe} \rangle \simeq 30 \quad \Rightarrow \quad \alpha_{PMT}^2 \simeq 0.4\%$



Appendix

Detector signal noise example:

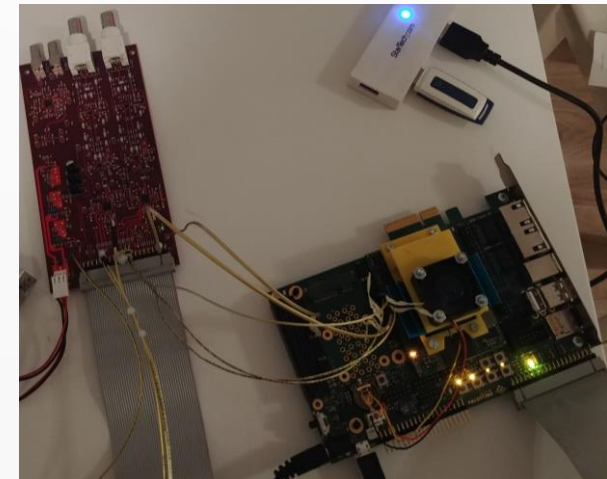
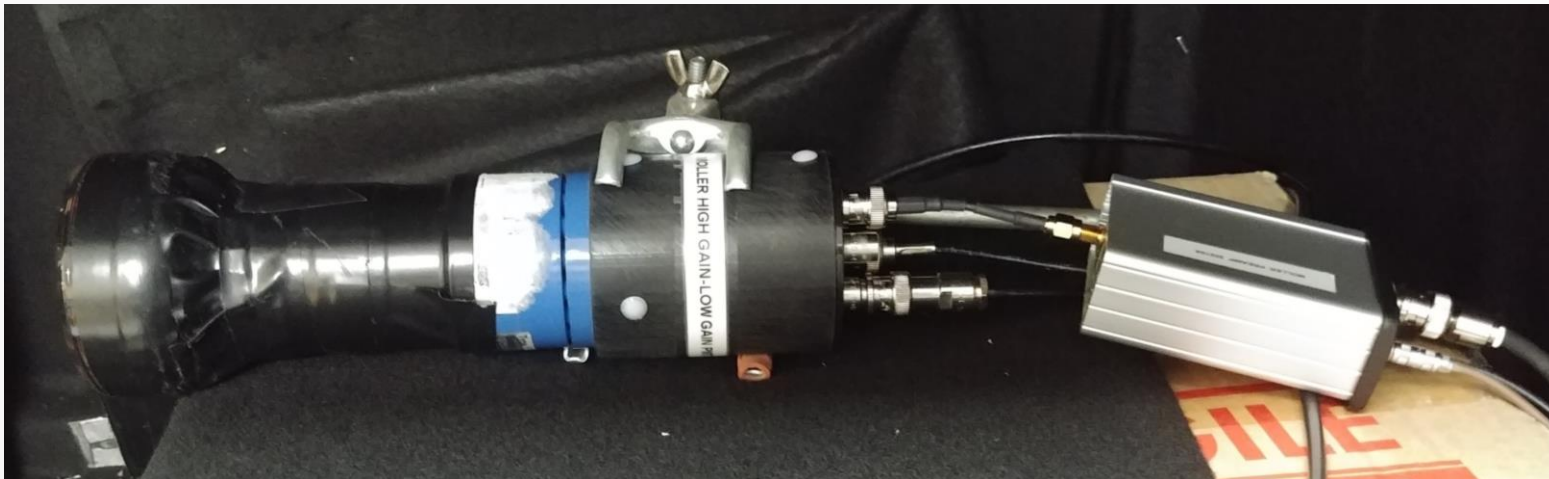
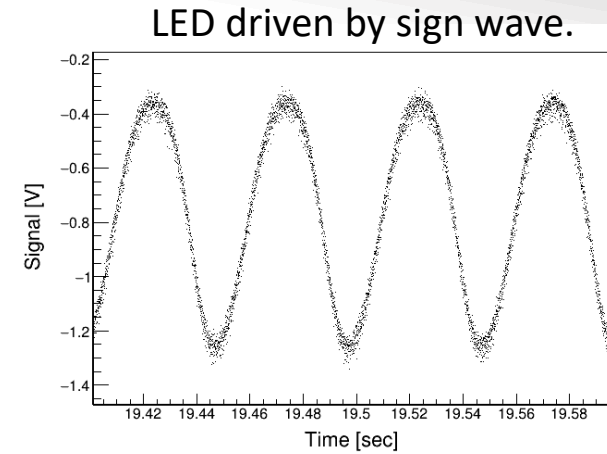
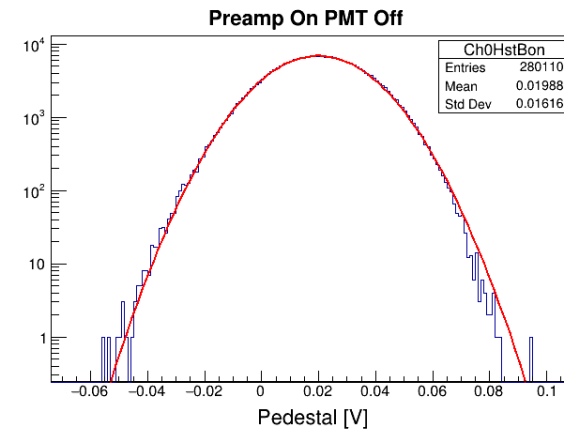
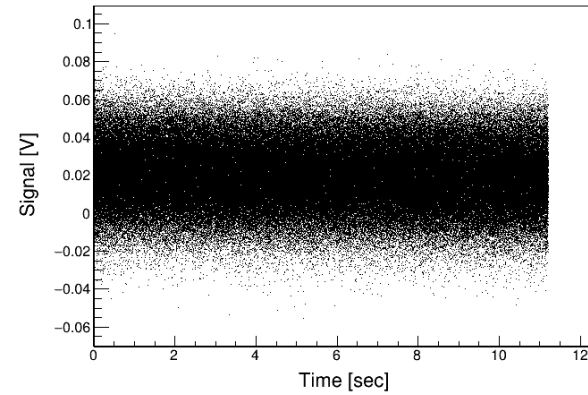
- Helicity settle time $10 \mu\text{s} \Rightarrow f_{3db} \approx 150 \text{ kHz} \Rightarrow \frac{\pi}{2} f_{3db} \approx 240 \text{ kHz} \Rightarrow B \approx 1 \text{ MHz}$
- Average cathode current: $I_c \approx 24 \text{ nA} \Rightarrow I_a \approx 12 \mu\text{A}$ with a gain of $g_{PMT} \approx 500$
- 3 stage PMT: $V_{bias} = 800 \text{ V} \Rightarrow V_{c,d1} = 270 \text{ V} \Rightarrow V_{d,d} = 178 \text{ V} \Rightarrow \delta_{d1} \approx 9, \delta_d \approx 7$
- PMT noise: $\alpha^2 \approx 0.004$ (nominally negligible)
- RMS in the PMT signal: $\sigma_a = \sqrt{2QI_a} \approx 240 \text{ pA}/\sqrt{\text{Hz}}$
- Preamplifier: at $g_{amp} = 250 \text{ k}\Omega$ and $B \approx 1 \text{ MHz} \Rightarrow V_{amp} \approx 3 \text{ V}$ and $\sigma_{amp} \approx 60 \text{ mV}$
- ADC resolution and noise: $\Delta = \frac{V_{ref}}{2^{18}} \approx 16 \mu\text{V} \Rightarrow \sigma_{dig} = \frac{\Delta}{\sqrt{12}} \approx 4.5 \mu\text{V}$
- ADC non-linearity (max values): $INL = 3 \text{ LSB} \approx 48 \mu\text{V}$, $DNL = 1 \text{ LSB} \approx 16 \mu\text{V}$
- Signal spread across ADC bins: $\frac{60 \text{ mV}}{\text{LSB}} = \frac{60 \times 10^{-3}}{16 \times 10^{-6}} \approx 3750 \text{ bins}$



Appendix

Beam and benchtop electronics tests

Integration mode tests with PMT illuminated by an LED:



PVES Measurements

The QWeak Experiment $Q_W^p = 1 - 4 \sin^2 \theta_W$

Measure A_{PV} as a function of electron helicity

Average Q^2 :	$0.0249 \pm 0.0006 \text{ GeV}^2$
Beam Energy:	$1.154 \pm 0.003 \text{ GeV}$
Beam Current:	$145 \mu\text{A} - 180 \mu\text{A}$
Beam Polarization:	0.89 ± 0.018
Target Power:	2.5 kW
Luminosity:	$1.7 \times 10^{39} \text{ cm}^{-2} \text{ s}^{-1}$
Integrated Rate (per detector):	875 MHz (7 GHz total)
Acceptance averaged asymmetry:	-0.23 ppm (nominal)
Standard Model:	$Q_W^p(Q^2 = 0) = 0.0713 \pm 0.0008$

Results (Nature volume 557, pages 207–211 (2018)):

$$A_{PV}(\vec{e}, p) = -226.5 \pm 7.3(\text{stat}) \pm 5.8(\text{sys}) \text{ ppb}$$
$$Q_W^p = 0.0719 \pm 0.0045$$

